Projecte Fi de Carrera

Enginyeria Tècnica de Telecomunicació
Especialitat en Sistemes Electrònics

GNSS signal detection based on first-order absolute statistics

Pau Buch Cardona

Director: José Antonio López-Salcedo

Departament de Telecomunicació i Enginyeria de Sistemes

Escola d'Enginyeria
Universitat Autònoma de Barcelona (UAB)

Setembre 2011

El sotasignant, *José Antonio López-Salcedo*, Professor de l'Escola Tècnica Superior d'Enginyeria (ETSE) de la Universitat Autònoma de Barcelona (UAB),

CERTIFICA:

Que el projecte presentat en aquesta memòria de Projecte Fi de Carrera ha estat realitzat sota la seva direcció per l'alumne *Pau Buch Cardona*.

I, perquè consti a tots els efectes, signa el present certificat.

Bellaterra, *1 de setembre de 2011*.

Signatura: *José Antonio López-Salcedo*

Vull agrair a José Antonio López Salcedo, el meu director de projecte durant aquests mesos, per haver-me ajudat i guiat a dur a terme aquest treball, com també per la correcció en el tema lingüístic que sense ell no hauria estat possible.

També vull agrair a la meva família per la paciència que han tingut durant aquests mesos, i per haver-me donat suport moral en tot moment. Espero tornar-vos-ho algun dia.

Contents

List of Figures

Chapter 1

Introduction

1.1 Motivation and Objectives

GNSS (Global Navigation Satellite System) has become more and more indispensable for many applications in all sectors from navigation positioning and smartphone utilities, to cartography and geodesy, modern agriculture or even in more critic situations such as hiking rescues. Some of them require a high positioning accuracy under harsh environments in order to work properly according to the requirements, but GNSS was first designed to work outdoors in open spaces.

Precision can be achieved using Differential GNSS but sometimes is not available when there is need to use them under environments where the received signal is too weak or there is a high noise component. This limitation can be due to the unavailability of having an extra receiver which is the positioning reference of the user's receiver. Besides, it has to be a data link between both receivers in order to be aware of arranged errors, provided by the reference receiver.

Another option is to use HS-GNSS (High Sensitivity GNSS) which have some specific acquisition blocks which help to find the signal amplitude by increasing the signal amplitude in reception. These specific blocks despite of being of great help, have their complexity in terms of computational load, due to large correlations, long integration times and large searching dimensions in order to find the signal peak. The possibility to improve the signal detection could be crucial in some situations because it improves the robustness of the receiver and allows it to extend its functionality to working scenarios where it was not originally designed to operate.

The main objectives of this project are:

- Use traditional second-order statistics with already known statistics to characterize signal detection metrics.

- Use first-order absolute statistics as another option in signal detection. Using new ap-

proximate closed-form expressions, characterize first-order absolute statistics to find the corresponding detection metrics.

- Compare both first-order and second-order absolute statistics performances in terms of receiver's performance to determine when the proposed detector, based in first-order absolute statistics, outperforms conventional receivers.

1.2 Description

This project can be fundamentally defined in three blocks.

The first one will define what is the process followed by conventional receivers in signal detection. Second-order statistics involving signal acquisition will be studied for the ideal searching case as a platform for the real situation in parallel acquisition. Theoretical concepts such as Extreme Value Theory and detection metrics will be first defined to be aware of them. At the end, all these concepts will be used to describe the detection performance of conventional receivers.

The second one will be centered in the use of first-order absolute statistics instead of second-order statistics. It will also be discussed its features in the ideal case of single time/frequency search as a basis of the actual case found in practice in multicell search. To do so, first-order absolute statistics will be studied and some closed-form expressions will be used to define these statistics and its performance in detection metrics. Finally, detection performance based in these new closed-form expressions will be compared with empirical evidences to make sure that it has been used reliable approximations.

The third one will compare both first and second-order statistic performances by comparing ROC (Receiver Operating Characteristic) curves. Both detectors will be compared working under many environment situations and different parameters set. That will give a wide vision of differences in performance and will allow classifying the best detector for each situation.

Finally, conclusions will be extracted in order to have a general idea about the performance of first-order noncoherent detector and its performance against conventional detectors.

Chapter 2

Fundamentals of GNSS

2.1 Introduction to GNSS

Global Navigation Satellite Systems are commonly known as GNSS, and allow users to be positioned from anywhere in the world with a great precision on the order of a few meters, or even less, depending on the working conditions. The first developments in satellite navigation systems were made by the US military, resulting in a system called Transit in the 1960s. It was based on exploiting the Doppler effect, where 6 satellites were put in orbit. By monitoring the frequency shift between transmitted and received one, it was possible to determine a particular position with not quite complexity. However, the low number of active satellites did not provide all-time-coverage. Because of the limitations of the Transit system, and due to technological war with the URSS, the USA government decided to begin the biggest project until the date in order to get the satellite navigation system leadership. A total of 24 satellites were put in orbit by the end of august 1993 paving the way for which it is currently known as the Global Positioning System (GPS), certainly the most popular of all GNSS systems.

Once a brief historical introduction has been made, we will introduce how modern GNSS works. It is important to make clear that this project assumes GPS as the navigation system chosen. The reason why, is because it has been the most used available navigation system in recent years for all kind of products, and it is still the only fully-operational system with global coverage.

2.2 GPS signal

The satellite signals which civilians are allowed to use are the C/A code (Coarse/Acquisition code) and the data modulated on the L1 carrier. Almost all GNSS products work with these two

parameters. L1 carrier is fixed to 1575.42MHz, as that is the frequency synthesized by atomic clocks on the satellite. Also BPSK modulation is transmitted, so that navigation bits are 1 or -1. As all satellites are transmitting into the same bandwidth, some medium access control (MAC) mechanism is needed to make them unique in some manner and avoid interference. That is the reason why it is used Code Division Multiple Access (CDMA). That means that every single satellite has a specific pseudorandom code, orthogonal with other satellite codes. These codes will allow the receiver to identify the responsible satellite for the signal received. Every code is a binary sequence of 1023 bits called chips and have duration of $977,52$ns everyone (T_c), which implies a total duration of 1ms

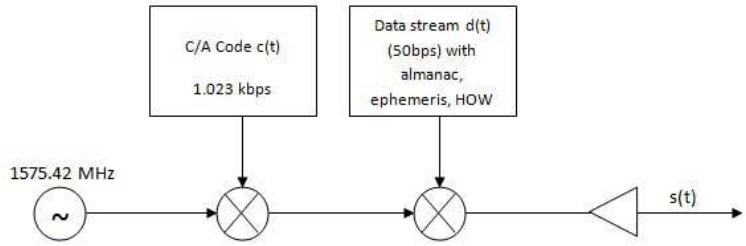

Figure 2.1: GPS signal generation at the satellite

This signal is again modulated by a 50bps datastream (same to say 20ms per bit, T_b) containing the ephemeris data and other important information needed in reception, shown in Fig. 2.1. The process of modulating a low data rate signal with a high chip rate pseurandom code is known as is known as DSSS (direct sequence spread spectrum). The resulting signal $s(t)$ has a new bandwidth of

$$BW = BW_{d(t)} \cdot \frac{T_b}{T_c} \tag{2.1}$$

being T_b/T_c the Processing Gain.

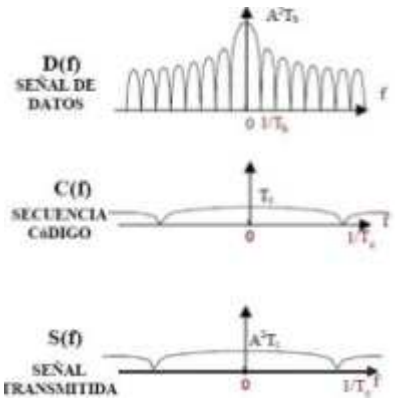

Figure 2.2: $d(t)$, $c(t)$ and $s(t)$ signal spectrums [Roi03]

An important feature of this procedure is that the total power spectrum in $s(t)$ is quite low

as it can be seen in Fig. 2.2. Some advantages of DSSS signaling are the following:

- Resistance to interferences (jamming, other satellite signals, multipath etc.).
- Being undetectable to undesired users, caused by reducing the total power transmitted.
- Accurate measures of propagation delay in reception (indispensable when calculating pseudorange values).

These pseudorandom codes are the already mentioned C/A codes, which belong to the family of Gold codes. In particular, Gold codes with a length of 1023 chips are adopted in GPS and more details about this codes and their properties can be found in [Tsu05].

After all this signal processing is done, the signal is sent to the Earth's surface. When arrives, in 77ms approximately, it is processed by the receiver which can begin to find the pseudorange values, needed to finally calculate the user's position.

2.3 Basic GNSS receiver

When the satellite signal arrives at the antenna, it is first amplified by a low noise preamplifier with the aim of making it perceivable to the rest of receiver blocks. Then, it is down-converted to IF (intermediate frequency) by the radio frequency front end. Normally, this intermediate frequency varies within the range of 2 to 20MHz. That process and all the operations that the signal undergoes within the receiver, always adds some thermal noise to the signal. Once the signal is in IF, a mixer removes the carrier frequency so it is down-converted into a base band signal which is digitalized thank to an ADC, where the original binary code remains. After that, it is introduced to the acquisition block where the desired signal is searched among the other non-desired signals in order to give the first estimations of C/A code delay and Doppler shift. Once this process has been taken, tracking block will be able to identify code delay and Doppler shift frecuency more accuratelly, and will allow to rearrange these parameters following any change during the positioning.

The acquisition process will be discussed in Section 3.1 since it has a close relationship with the work done in this project. To read more about the other signal processing blocks, [D.K06] would be a good reference.

2.3.1 Acquisition process

Once the processed signal goes out from the mixer, it finds the coherent correlator. The job of the coherent correlator is to find the satellite signal among the disturbing noise. The processed

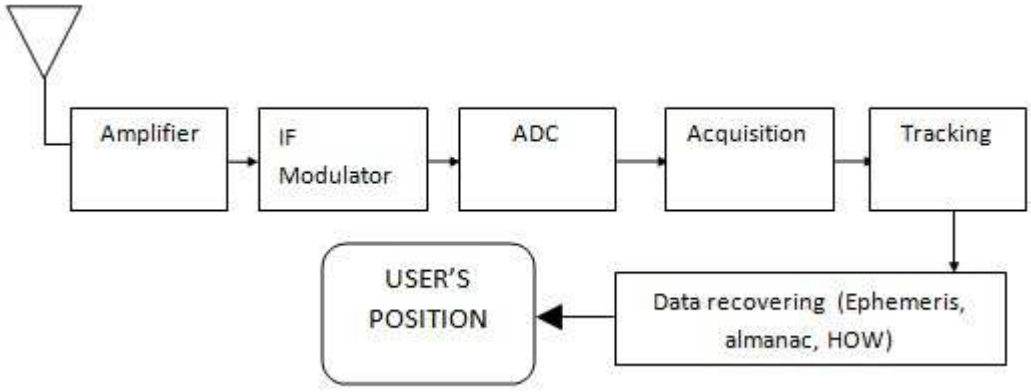

Figure 2.3: Simplified diagram block of a GNSS receiver

signal after the mixer is

$$r(t) = A \cdot s(t-\tau)e^{j\omega_d(t-\tau)} \tag{2.2}$$

where A is the amplitude from the transmitted signal $s(t)$, τ is the corresponding C/A code delay, and ω_d the Doppler frequency shift.

The correlator in Fig. 2.4 is in charge of multiplying the noisy signal $r(t)$ with the code of the satellite under analysis. After that, the multiplied values are integrated. For the case of being aligned, this value turns out to be a large number compared with the situation when the noisy signal does not contain satellite data or when it is not aligned. In that case, the resulting integration will tend to 0 because the resulting multiplied signal tends to be again a noisy signal with zero-mean.

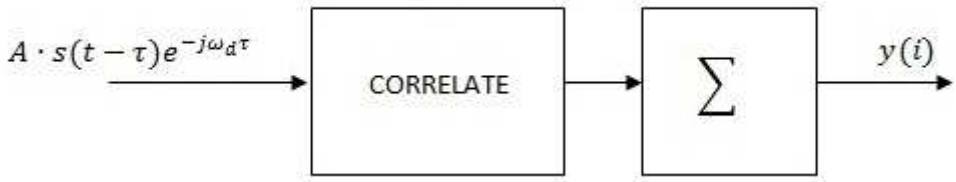

Figure 2.4: Acquisition correlator

In multicell search (Section 2.3.2), once the acquisition matrix has been filled with the corresponding correlation values, the maximum of them is picked up. This value has to be compared with a threshold to determine whether the signal processed was from the satellite (hypothesis $\mathcal{H}_1$) or just noise (hypothesis $\mathcal{H}_0$). More information about statistics involving taking the maximum value, will be explained later on in Section 2.6. Regarding the two hypotheses, in

order to be distinguished, $\mathcal{H}_0$ and $\mathcal{H}_1$ can be both defined as

$$\mathcal{H}_0 \quad : \quad x[n,i] = w[n,i] \tag{2.3}$$

$$\mathcal{H}_1 \quad : \quad A \cdot e_n^{j\omega_d} + w[n,i] \tag{2.4}$$

The term ω_d is due to the granularity of the search process undergone at the acquisition stage. If Doppler bins were arbitrarily small, the error would tend to 0. This phase varies every time. Sometimes it is need to sum many samples with varying phase. If the resulting phase overcomes 2π, the resulting signal turns out to have less amplitude than the expected (depicted in Fig. 2.5). This phase phenomenon is known as phase wrapping and it is schematically represented in Fig. 2.5.

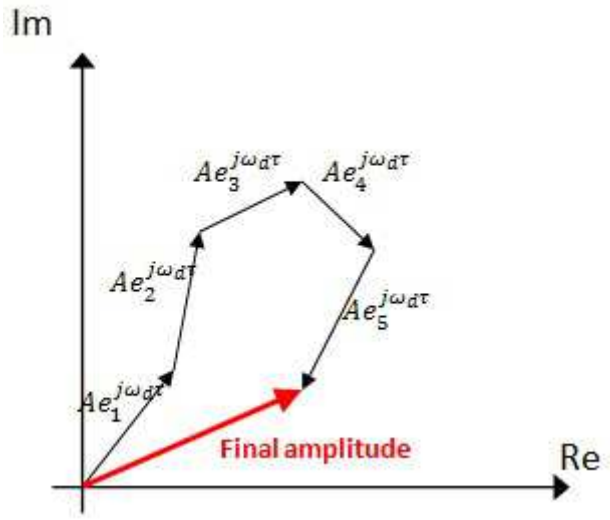

Figure 2.5: Phase wrapping

If the extreme value under $\mathcal{H}_1$ hypothesis surpasses the threshold, the next step is the tracking block and recover the navigation bits. However, sometimes the value found after picking the maximum cell from the acquisition matrix, despite being under hypothesis $\mathcal{H}_1$, does not exceed the threshold, so the satellite signal is misdetected. In order to circumvent this issue, more coherent integrations should be taken and sometimes it is needed to combine them with noncoherent integrations. Both concepts are explained in Section 2.5.1.

2.3.2 Acquisition strategies

When finding satellite signal, after being processed by the mixer, there are two issues which make it difficult; C/A code delay and Doppler frequency shift as a consequence of satellite's movement.

Assuming that these inconveniences do not exist, the only thing the receiver needs to do

is to correlate the $r(t)$ signal with the local code and make as many coherent integrations as it is needed (Section 2.5). Once the result is obtained, the receiver just has to compare this value with the threshold to decide whether it is under $\mathcal{H}_0$ or $\mathcal{H}_1$ situation. In this project, the assumption of not having neither Doppler frequency shift nor C/A code delay uncertainty will be treated as **Single cell search**. Despite it is an ideal situation and it cannot be found in any real case, it will be studied in order to help to understand the complex case which is the found in GNSS receivers.

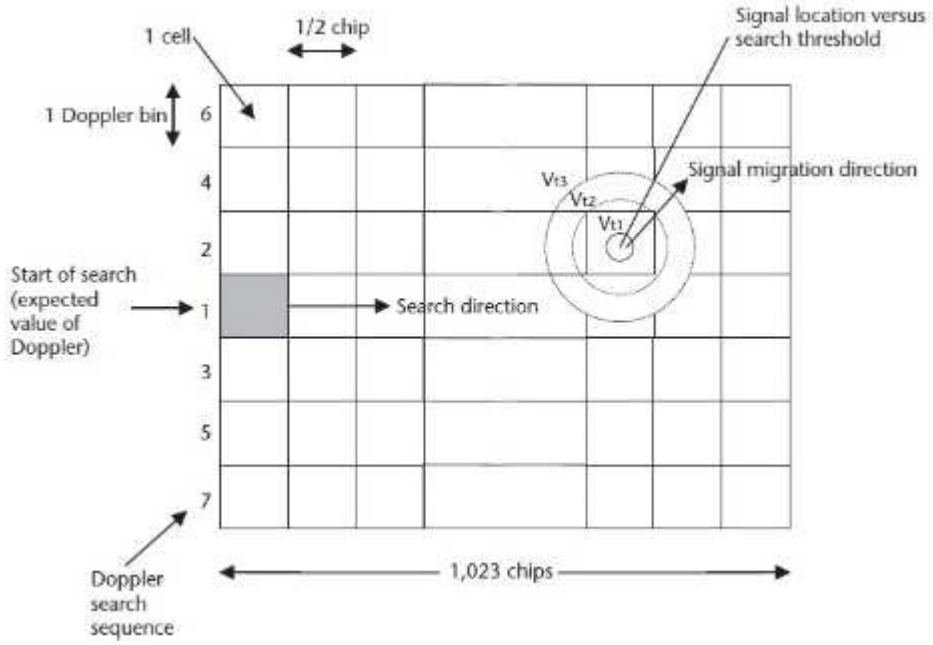

Figure 2.6: Multi cell matrix acquisition [D.K06]

On the other side, the actual case found in practice deals with some issues which make finding the satellite signal a challenging procedure. It will be called **Multicell search**, and it will be also studied in the following chapters.

In order to find the corresponding C/A code delay and Doppler frequency shift, the search is based in an acquisition bidimensional matrix depicted in Fig. 2.6. In the x axis, it is replicated all 1023 C/A code phase. In the y axis, Doppler shift range, which should cover the majority of possible values. The code phase is searched in increments of 1/2 chip, and every increment is called code bin. On the other side, Doppler frequency shift is also divided in bins which typically vary from 67Hz for strong signals, or 667Hz for poorer ones.

The first fix search begins considering non code delay and the mean Doppler frequency shift as the starter point. Once it has been looked for all possible code delays, Doppler bin changes at time until the satellite signal is found or the search finishes without desired results. In that case, the estimated code should be changed for another candidate. If it is wanted to read more

about the matrix acquisition, [Dig09] would be a good reference.

2.3.3 Acquisition issues

The received signal from GPS satellites is very weak because of the long way between their orbit and the Earth's surface (about 22000kms). This limitation affects the acquisition process made by GNSS receivers. If the acquisition is made indoors, this handicap increases from 10 to 1000 times more.

Another limitation is the slow startup sequence where the acquisition time spends approximately 1 minute long to the first fix. After this first scan, a position can be computed every second. In order to be positioned, ephemeris data need to be recovered from satellites signal, which will help to determine the satellite orbits and clocks.

An already listed acquisition issue was the term $e_n^{j\omega_d}$ accompanying the amplitude after the correlator. That was the time-varying phase introduced by the residual carrier frequency error, as a result of the acquisition process, where phase derives from Doppler shift could not be eliminated. This phase can be very harmful when correlation peaks are summed in order to have a greater final amplitude, because this varying phase can cause a disminution of the resulting signal. This effect, which is known as phase wrapping, is schematically depicted in Fig. 2.5.

These issues can be circumvented using HS-GNSS (High Sensitivity GNSS), as it will be seen in Section 2.5. If it is not enough, A-GPS (Assisted GPS) may be needed. This project is developed under the assumption of working with a HS-GNSS.

2.4 Working scenarios

As it has been seen, one of the varying handicaps while signal acquisition is the low power received in reception. To cope with this issue, first of all, it has to be identified and classified. The way to determine the quality of the received signal in front of the noise added, is similar to the one used in other communication systems (SNR). This metric is called C/N_0 (Carrier-to-Noise ratio) and gives a similar information as SNR. The advantage of using C/N_0 instead, is that it does not have a relationship with the receiver's bandwidth, so classifying the quality of the signal this way, C/N_0 can be used for all kind of receivers, having the same meaning to all.

It is need to distinguish from 4 possible situations depending on the C/N_0 in reception:

- **Outdoor scenario** is within the C/N_0 range which receivers usually work. This slot is compressed between 45-35 dBhz. It is a LOS (Line Of sight) situation, which implies that there are no obstacles between the transmitter and the receiver.

- **Soft indoor scenarios** are compressed between 35 and 25dBhz. They are typical situations near buildings, under foliage, where there might not be a line of sight. Within in this range, receivers lose accuracy and may stop working properly.

- **Indoor scenarios** from 25 to 10dBhz. In these situations, there might be attenuations on the order of 3dB per meter when moving in from outside wall [Pet97]. Conventional GNSS receivers cannot work here. Using HS-GNSS may be the solution as they use a large coherent integration period combined with a particular number of non-coherent integrations, so the total amplitude given by same C/N_0, is greater than conventional receivers. However, the message brought in the signal cannot be recovered, so Assisted GNSS may be needed in order to find user's position.

- **Deep indoor** are the toughest enviroments when the C/N_0 ratio is below 10dBhz. Here, it is hardly possible to be positioned. The majority of GNSS receivers do not even recognize whether is there signal or not. Theorically it might be possible but the user could not have a real time positioning because of the magnitude of the calculations needed. That is the typical situation found when being inside a building or into a tunnel.

The work done in this project has been based in C/N_0 values according to the pattern listed before.

2.5 HS-GNSS receivers

HS-GNSS work with the same procedure as conventional GNSS receivers but they have some specific acquisition blocks to guarantee proper final signal amplitude in order to detect the majority of H1 situations.

The best acquisition process would be the situation where the incoming signal is correlated by the 1ms long C/A code, obtaining a great peak of correlation. What it cannot be avoided is the correlation of the noise added to the incoming signal with the local code. Despite of this issue, if the resulting peak is greater than the noise's amplitude, there would not be problems to distinguish both situations, and make the comparison with the threshold more efficient.

To achieve this benign situation, GNSS receivers have coherent integrators which sum many output correlation peaks to increase the total amplitude. At the same time, the disturbing noise is also summed. However, this noise signal with zero-mean, does not increase.

Coherent integrations are not always enough to guarantee proper signal amplitude. The maximum coherent integrations are limited to 20ms as it is the same of 20 correlation peaks.

That is because after the 20ms, the navigation bit can change, so the correlation peak can turn its amplitude to negative (if navigation bit is -1). That turns against the coherent integrations because instead of summing peaks, they would be subtracting amplitude. Also phase derives can reduce the accumulated amplitude as it is has been explained in section 2.3.3

2.5.1 Noncoherent integration

In order to circumvent these limitations, the result of coherent integration is put through a nonlinear function and then is integrated, as it can be seen in Fig. 2.7. This nonlinear function, typically consists on squaring the output value $y(i)$, for the majority of receivers. As it is known, when applying the absolute moment to a phasor, phase disappears but module remains. That allows summing the coherent correlation peaks without neither phase problems nor navigation changing bits.

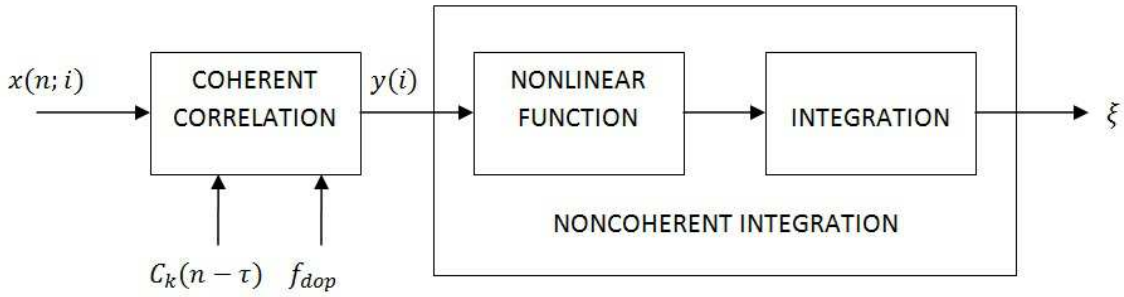

Figure 2.7: Acquisition module in HS-GNSS

The process of applying a nonlinear function to $y(i)$ and then integrate it, is called noncoherent integration. This combination between coherent and noncoherent integrations is the method used by HS-GNSS. With this technique, the possibility of having higher amplitude values when comparing it with the threshold is achievable.

Always benefits have their limitations. The more noncoherent integrations taken, the more acquisition time is spent. That could affect the first fix time, which could be elongated too much if the receiver's features are not enough to support the requirements.

As it has been said, second-order nonlinear functions are the most used. The main reason of their use is because second-order statistics involving a random variable, as the resulting value ξ, are well known as square-statistics. This statistics provide good detecting results, so that is the reason why their operability has not been questioned yet.

Some recent studies, have shown that other n^{th} order statistics may outperform the actual system such as absolute moment instead of the second [LS08b].

2.5.2 New acquisition proposals

As it has been said, within the acquisition process, the most critical part is when the receiver has to find satellites the first time, the first fix. The majority of receivers, have their operational threshold around $C/N_0 = 33 - 35$ dBhz and HS-GNSS are expected to work behind them (from $10 - 25$ dBhz). Working in that range, they are forced to have long correlation periods which let them find the satellite signal. Conventional GNSS receivers usually use second-order statistics during the acquisiton process which have been found to be the optimal for Gaussian input signals. The problem appears when noise has similar amplitude to the desired signal because noise peaks can be mistaken for signal peaks.
To solve this problem, some crosscorrelation between input signals, reduces the total signal noise and sensitivity increases, using second-order statistics. Some hybrid methods using both differential correlation and squared envelopes have been developed and it has been seen that outperform second-order integrations.

Although all these improvements, second-order statistics may not be the best nonlinear function for all situations. Other nonlinear functions may overcome the performance offered by second-order statistics. An alternative to cope with the noise-level problem is the use of the metric based on the nonlinear function which becomes to be

$$\xi_\alpha = \sum_{i=0}^{N_i-1} |y(i)|^\alpha \,. \tag{2.5}$$

being α a constant between $(0, 1]$. The statistics involving this new metric are called FLOS (fractional lower-order statistics). Some comparisions in [LS08b] have been made and FLOS have been found to provide best performance, concretely $\alpha = 0.7$ and $\alpha = 0.8$ for PFA> 0.05, but for lower values, $\alpha = 1$ overcomes the other options.
Despite these FLOS would make the receiver perform better, statistics involving them are unknown. That is why second-order statistics are still unbeaten in detection use.

Based in this assumption, this project is going to face the possibility to stablish some formulae for new metric with $\alpha = 1$ and compare the results obtained with the performance of second-order noncoherent detectors. To read more about this study and look for some results, [LS08b] might be consulted.

2.6 Extreme Value Theory

Returning to the acquisition process, and more specifically to multicell search, it has been seen that every cell was filled with noise or signal plus noise (only in one cell, as it is the specific Doppler shift-code delay combination where satellite signal stands). Once this matrix was filled,

it was taken the maximum value among all cells. Well, this trivial thing has a consequence involving statistics.

Every value in each cell is a random variable (r.v.). That is because the noise added in reception, was a Gaussian random variable with zero-mean and $\sigma^2 = 1$. Whether or not containing satellite signal, every cell has a noise component that fix them as gaussian r.v.
The picked value remains as a random variable but its statisticals changes. The decision of picking the maximum value from a set of random variables, follows a well-known statistic theory. This theory is based on the extremal types theorem, also called the three types theorem, stating that there are only three types of distributions that are needed to model the maximum or minimum of the collection of random observations from the same distribution [Emb97, Chap. 3].

As it can be read in [Tur07], dealing with exponential decreasing tail distributions as Gaussian, the CDF (F_n) of the limiting distribution has the double exponential form

$$F_n(x) = \exp(-\exp(-\alpha_n(x - u_n))) \tag{2.6}$$

where x is the maximum output value from all matrix acquisition's cells, which everyone comes from the noncoherent correlator exit (ξ') in Fig. 2.8.

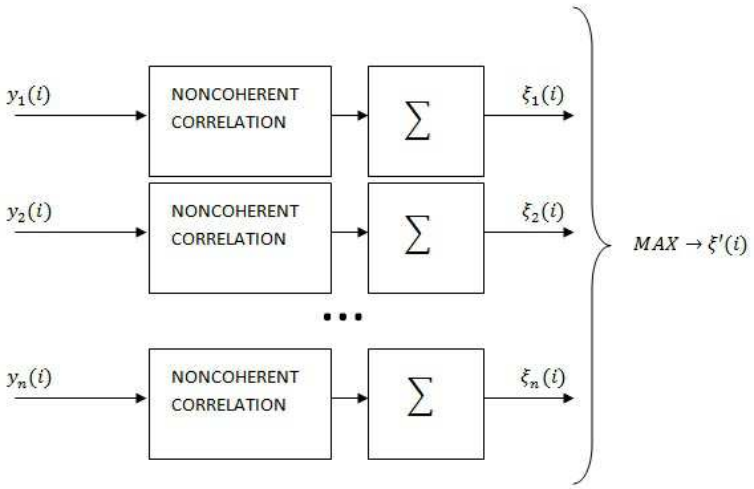

Figure 2.8: Maximum output value from noncoherent correlators

Coefficients u_n and α_n are defined by the equations

$$F(u_n) = 1 - \frac{1}{n} \tag{2.7}$$

and

$$\alpha_n = nf(u_n) \tag{2.8}$$

being $F(x)$ and $f(x)$ the CDF and PDF (probability density function) of the n independent and identically distributed random variables which form the acquisition matrix (n tending to infinity).

2.7 Fundamentals of Detection Theory

As it was first explained in acquisition process in (Section 2.3.1), when the maximum value is picked, it has to be compared with the threshold. The resulting decision will consider if the received signal was the expected one, and will only distinguish the two possible options ($\mathcal{H}_1$ and $\mathcal{H}_0$). At first sight, it could be thought that these two options are the only two possible situations after the decision. Notwithstanding, there are more possible detection results which are as follow.

- **True Positives**. Receiver considers being under $\mathcal{H}_1$ hypothesis. The value chosen is also the satellite signal bin.

- **True Negatives**. Receiver considers being under $\mathcal{H}_0$ hypothesis. The value chosen is a noise bin and it does not overcome the threshold.

- **False Positives or False alarm**. Receiver considers being under $\mathcal{H}_1$ hypothesis. The value chosen is a noise bin but it is considered satellite signal by the receiver because it exceeds the threshold.

- **False Negatives or Misdetection**. Receiver considers being under $\mathcal{H}_0$ hypothesis. The value chosen is the satellite signal bin but it does not exceed the threshold, so it is misconsidered $\mathcal{H}_1$ (typical found in indoor scenarios).

From these possibilites can be defined three more fundamental ideas in order to characterize the acquisition process.

- **Probability of Detection** (P_d). Is defined as the probability of the receiver to successfully detect the presence of satellite signal when it is searching under the hypothesis $\mathcal{H}_1$. That would consider True Positives. It can be also statically defined as the right tail integration of the signal plus noise distribution, from the threshold chosen.

- **Probability of False Alarm** (P_{fa}). Is defined as the probability of the receiver to wrongly consider the presence of satellite signal when searching under hypothesis $\mathcal{H}_0$. That would consider False Positives. It has also an statistical definition which is the right tail integration of the noise distribution, from the threshold chosen.

- **ROC curve**, which stands for Receiver Operating Characteristics. It is a graph which allows the user to depict the tradeoff between true positive rates and false alarm rates of classifiers and it has been long used in detection theory [Ega75] . The ROC curve will be calculated in order to determine receiver's features and to let the reader compare different performances depending on the detection technique under analysis.

Finally, the last definition must be done. The first goal of any detector, is to maximize the probability of detection. That implies to set a threshold (γ). All the values which overcome this threshold, are been considered under $\mathcal{H}_1$ situation. The better option would be not missing any satellite signal values (Which is the same to say, none False Negatives). That means that the threshold has to be set to 0, and implies $P_d = 1$. However, all False Positives would be also picked and $P_{fa} = 1$. What is really wanted from a good detector, is to maximize the probability of detection for a determined probability of false alarm. So the final commitment to set the threshold's value, is to fix the P_{fa} and maximize the P_d [Kay98].

Chapter 3

Traditional GNSS signal detection based on second-order statistics

In this chapter, second-order absolute moment acquisition is going to be analysed for both acquisition strategies. The single cell search will be the first one to be defined as it contains basic statistical concepts which will be applied in multicell acquisition. Both strategies will be placed in different working scenarios to have a wide vision of their implementation.

Once their statistics have been analysed, detection features such as Probability of Detection, Probability of False Alarm and ROC curve will be given. Despite single cell search do not really correspond to a real implementation, P_d, P_{fa} and ROC curve will be also shown in order to compare them with the actual case found in practice. That is made to be aware how statistics change when taking the maximum among a group of random variables.

3.1 Single cell analysis

Coming back to the GNSS block diagram in Fig. 2.7, the detection metric becomes

$$\xi = \sum_{i=0}^{N_i-1} |y(i)|^2 . \tag{3.1}$$

being $y(i)$ the value after coherent correlation and N_i the number of noncoherent integrations added.

The input signal $y(i)$, was previously defined as a Gaussian random variable. It was made of AWGN (Additive White Gaussian Noise) which has a distribution following a $\mathcal{N}(\mu, \sigma^2)$. In base band, this noise can be broken down into in-phase and quadrature components

$$\omega(n) = i(n) + jq(n) \tag{3.2}$$

Where $i(n)$ is the in-phase gaussian component following a $\mathcal{N}(0,\sigma^2)$, and $q(n)$ the quadrature Gaussian component which follows also a $\mathcal{N}(0,\sigma^2)$. σ^2, which is the noise power will be particularly assumed as 1 for the sake of simplicity. As C/N_0 will be fixed, if one of their components is also pre-determined, the other will be in tune with the C/N_0 expression.
So, returning to the ξ definition, $y(i)$ can be defined as

$$y(i) = \begin{cases} A \cdot e^{j\omega_d \tau_i} + \omega(i) & : \mathcal{H}_1 \\ \omega(i) & : \mathcal{H}_0 \end{cases} \tag{3.3}$$

For the $\mathcal{H}_0$ case, y(i) random variable will follow a $\mathcal{N}(0,\sigma^2)$ and for the $\mathcal{H}_1$ situation, this r.v. can be seen as a $\mathcal{N}(A,\sigma^2)$, being A the value amplitude achieved after the coherent correlator. It can be defined as

$$A = \sqrt{C/N_{0linear} \cdot T_{coherent} \cdot 10^{-3}} \tag{3.4}$$

For $\mathcal{H}_0$ case, ξ can be defined as a *central chi-squared i.i.d random variable* with a probability density function as it comes

$$f(x|\mathcal{H}_0) = \begin{cases} \frac{1}{2^{\frac{\nu}{2}}\Gamma(\frac{\nu}{2})} x^{\frac{\nu}{2}-1} \exp(1-\frac{1}{2}x) & x > 0 \\ 0 & x < 0 \end{cases} \tag{3.5}$$

With ν degrees of freedom, assume to be an integer defined as

$$\nu = 2 \cdot N_{intnoncoh} \tag{3.6}$$

It is important to remark why the number 2 appears in (3.6). When the input signal goes through the noncoherent integrator, both noise components become a central chi-squared i.i.d random variables. They are added together and that is why the sum of two chi-squared r.v. become another chi-squared r.v with 2 degrees of freedom.

The function $\Gamma(u)$ is the Gamma function appearing in (3.7), and is defined as

$$\Gamma(u) = \int_0^\infty t^{u-1} \exp(-t) dt \tag{3.7}$$

Under $\mathcal{H}_1$ hypothesis, ξ becomes a *noncentral chi squared r.v.* Its pdf turns out to be defined as

$$f(x|\mathcal{H}_1) = \begin{cases} \frac{1}{2}(\frac{x}{\lambda})^{\frac{\nu-2}{4}} \exp[-\frac{1}{2}(x+\lambda)] I_{\frac{\nu}{2}-1}(\sqrt{\lambda x}) & x > 0 \\ 0 & x < 0 \end{cases} \tag{3.8}$$

With ν degrees of freedom. λ is called the *noncentrality parameter* and it is defined as

$$\lambda = \sum_{i=1}^{\nu} \mu_i^2 \tag{3.9}$$

Whereas $I_r(u)$ is the *modified first-order Bessel function*.
Once the statistics have been defined, we are ready to compare both empirical and exact distributions in order to be sure about the exact expression with all parameters well-adjusted.

The empirical results have been obtained by generating data with Matlab. All the samples have been generated under the Gaussian distribution $\mathcal{N}(0, \sigma^2)$ simulating the original input samples. The data under $\mathcal{H}_1$ had an amplitude added in order to represent signal plus noise values. After that, the data was put through the acquisition blocks in order to have the resulting output values which were able to be depicted in order to compare them with the exact expressions. It has been very important to calibrate the empirical data generation, and also the way parameters are processed. That is done to be sure that there are no parameter errors between the exact formula and the empirical representation for posterior use.

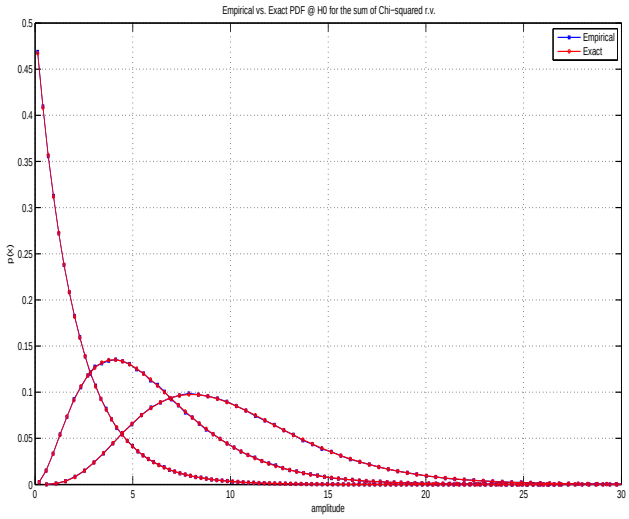

Figure 3.1: Empirical vs. exact PDF's @ H0 with N_i={1,3,5} and C/N_0=45dBhz

As it can be seen in Figs. 3.1 and 3.2, both empirical and exact distributions almost fit perfectly.

Once the verification has been done for the PDF, it is also required to double-check the tightness of the theoretical amb empirical cumulative distribution function (CDF). Figs. 3.3 and 3.4 show how both emprical and exact cdfs fit. Looking at these figures, it is important to make sure that values near 0 and 1 respectively fit as much as possible. That is because when calculating detection and false alarm probabilities, sometimes it is interesting to have one of them near these extreme values, so accuracy is required.

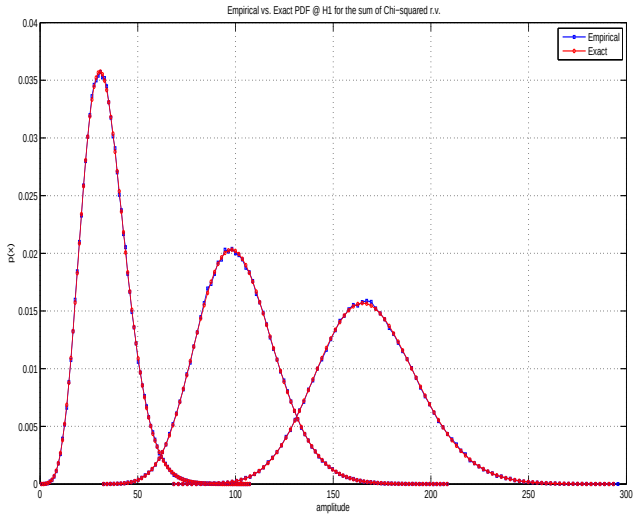

Figure 3.2: Empirical vs. exact PDF's @ H1 with N_i={1,3,5} and C/N_0 = 45dBhz

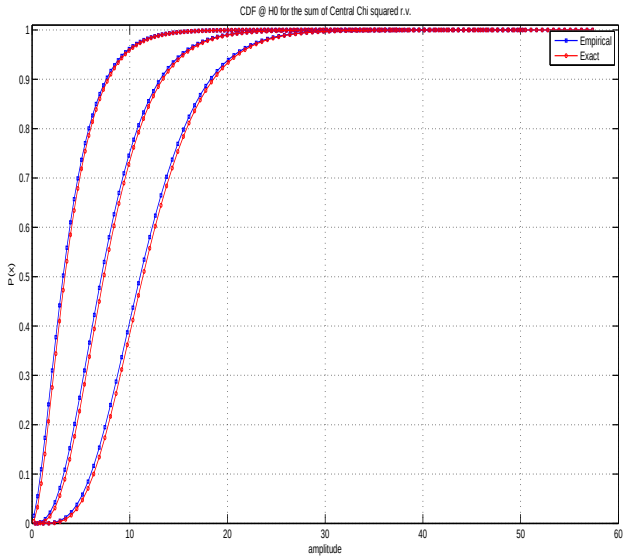

Figure 3.3: Empirical vs. exact CDF's @ H0 with N_i={2,4,6}

3.1.1 Detection metrics

Probability of detection was already defined in Section 2.7. So the right tail integration is from a Noncentral Chi-squared pdf in Fig. 3.2. P_d graphical representation is in Fig. 3.5.

On the other side, probability of false alarm will be the right tail integration from a Central Chi-Squared pdf depicted in Fig. 3.1.

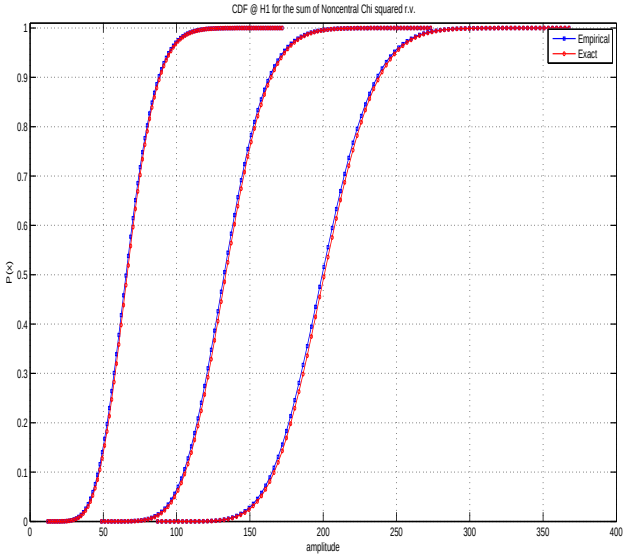

Figure 3.4: Empirical vs. exact CDF's @ H1 with N_i={2,4,6} and C/N_0 = 45dBhz

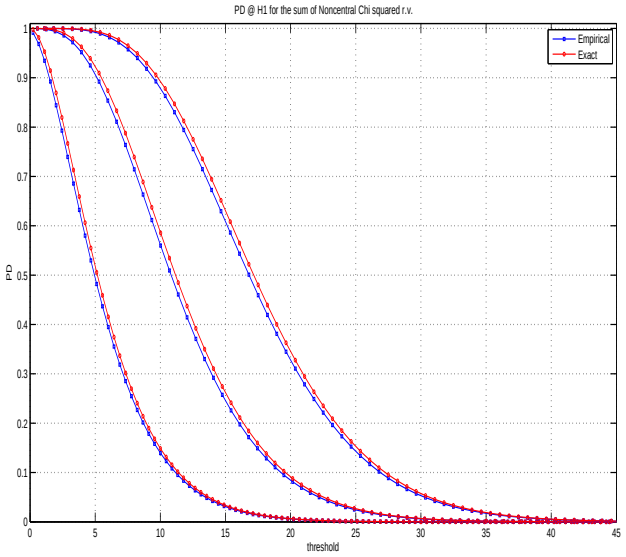

Figure 3.5: Empirical vs. exact PD's @ H1 with N_i={2,4,6} and C/N_0 = 30dBhz

Once the probability of detection and probability of false alarm have been defined and compared, it is time to compare the ROC curve.

One important feature like the capability of a receiver to detect the satellite signal, can be easily seen in ROC curves. The following figure in Fig. 3.7 is a clear example. The Acquisition process made with less noncoherent integrations has smaller noncoherent output (ξ) value amplitude. They can be easily misdetected or there is major probability to overcome the threshold (False

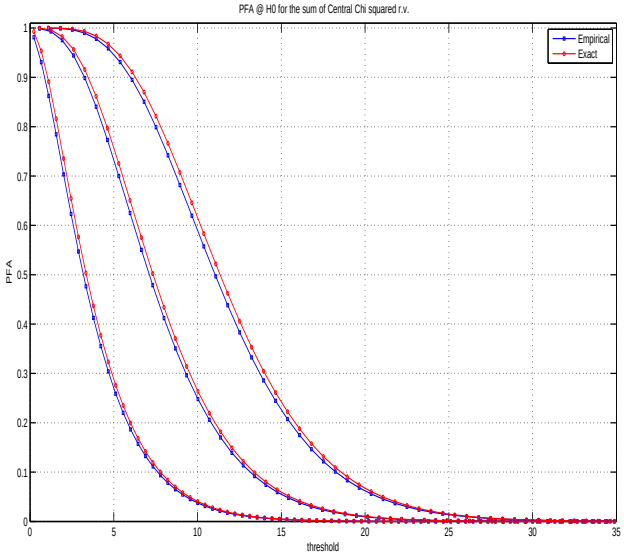

Figure 3.6: Empirical vs. exact PFA's @ H0 with N_i={2,4,6} and C/N_0 = 30dBhz

Alarm). With the ROC curve, this characteristic is easy to see. The process made with less noncoherent integrations, has not so sharper outside curvature than the ones which have more noncoherent integrations. Consequently, they have higher P_d for same P_{fa}.

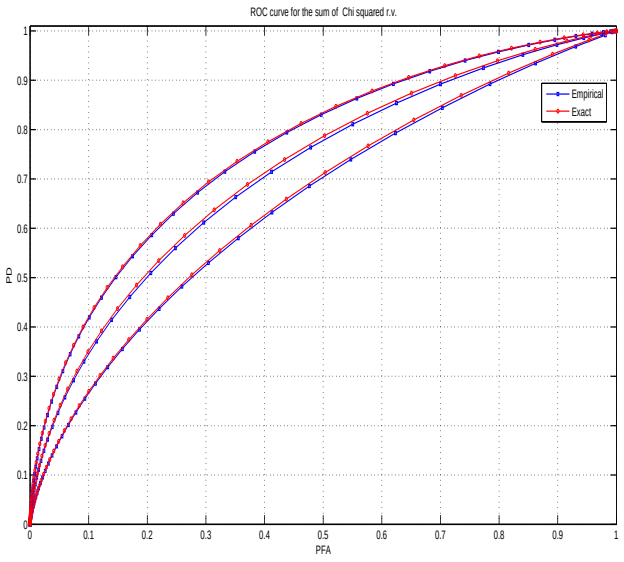

Figure 3.7: Empirical vs. exact ROC curves with N_i={2,4,6} and C/N_0 = 30dBhz

As it can be seen in Fig. 3.6, the more noncoherent integrations are there, the more $\mathcal{H}_0$ distribution tends to have a greater amplitude. That could be a kind of paradox because despite

of having greater amplitude, there are more chances to avoid false alarm for the same detection probability. That can be checked looking at Fig. 3.7. The explanation about that is very simple. At the same time $\mathcal{H}_0$ distribution was shifted to the right, noncoherent integrations did the same with $\mathcal{H}_1$ values, with the difference that $\mathcal{H}_1$ values were more enhanced than $\mathcal{H}_0$. This noncoherent correlation property was already given in section 2.5.1.

3.2 Multicell analysis

Moving forward to the actual case found in practice, parallel acquisition is the process found in GNSS receivers. When the maximum value from the acquisition matrix is picked up, statistics involving it become present [Emb97].

Receiver will be under $\mathcal{H}_0$ hypothesis if all bins from the acquisition matrix are exclusively noise. The opposite situation, hypothesis $\mathcal{H}_1$ will be present if at least one of the acquisition matrix cells, has signal plus noise. So, when talking about detection, it has to be understood that the satellite is present in one of the cells. Knowing the specific cell would imply another specific study, not considered in this project.

The statistics of each cell have been introduced in Section 3.1, and they are the basis for the statistics of the multicell detection strategy to be presented herein.
Being under $\mathcal{H}_0$ situation and having picked the extreme sample, the cumulative distribution (CDF) can be found going through the EVT formulae mentioned in section 2.6. This expression was

$$F_n(\xi') = \exp(-\exp(-\alpha_n(\xi' - u_n))) \tag{3.10}$$

The parameters, needed in this situation are

$$F(u_n) = 1 - \frac{1}{n} \tag{3.11}$$

and

$$\alpha_n = nf(u_n) \tag{3.12}$$

Where $F(u_n)$ is the CDF of ξ', evaluated in u_n, n is the number of cells composing the acquisition matrix, and $f(u_n)$ is the $\mathcal{H}_0$ pdf evaluated in u_n.

This pdf, turns out to be the one defined in (3.5). If the resulting CDF is graphically represented, turns out to be Fig. 3.8.
As it can be seen, the more noncoherent integrations added, the greater amplitude of the output noncoherent correlator is (also in multicell search).
The EVT better adjust between empirical and exact is found when the number of noise bins n

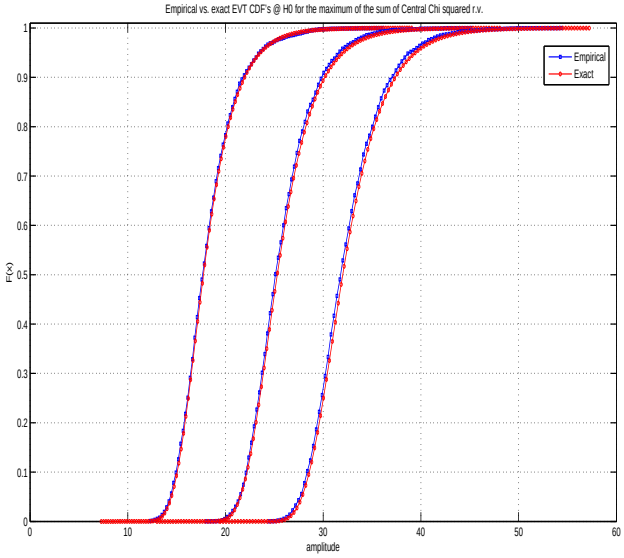

Figure 3.8: Empirical vs. exact EVT CDF's @ H0 with N_i={2,4,6} and C/N_0 = 30dBhz

tend to infinity, because indeed, the EVT applies asymptotically. In Fig. 3.8 it has been used 500 noise cells. For a better fitting, more noise cells should be considered.

$\mathcal{H}_1$ situation has more complexity, so it will be detailed properly below.

3.2.1 Detection metrics

Once $\mathcal{H}_0$ hypothesis is defined, probability of false alarm comes alone and it is defined as

$$P_{fa} = 1 - F_n(\gamma) \tag{3.13}$$

being $F_n(\gamma)$ the CDF corresponding to the maximum value among n samples from the acquisition matrix calculated in (3.10). P_{fa} can be graphically depicted as Fig. 3.10.

In order to define probability of detection, $\mathcal{H}_1$ statistics must be found.
In multicell acquisition, the EVT cannot be directly applied if the receiver is under $\mathcal{H}_1$ hypothesis. The EVT is exclusively referred to pick up the maximum value from identically distributed random variables. This is not the case concerning $\mathcal{H}_1$ hypothesis. It was defined as the situation were at least one of the acquisition matrix cells, had signal plus noise. The fact which implies having a cell different distributed to the rest, makes the EVT inapplicable.
Despite there is no closed-form distribution, some mathematical derivations allow us to calculate probability of detection directly without knowing the cumulative distribution. The mathematical expression for P_d is

$$P_d(\gamma) = \int_{\gamma}^{\infty} f(\xi'|\mathcal{H}_1)dz \tag{3.14}$$

$$P_d(\gamma) = \underbrace{\int_{\gamma}^{\infty} f_{X_{sat}}(\xi')F_{M_{n-1}}(\xi')d\xi'}_{detection} + \underbrace{\int_{\gamma}^{\infty} f_{M_{n-1}}(\xi')F_{X_{sat}}(\xi')}_{misdetection} \tag{3.15}$$

where $f(\xi'|\mathcal{H}_1)$ is the unknown distribution involving $\mathcal{H}_1$ hypothesis for the maximum value (ξ'). $f_{X_{sat}}(\xi')$ and $F_{X_{sat}}(\xi')$ are the pdf (3.8) and cdf from the signal cell. $F_{M_{n-1}}(\xi')$ and $f_{M_{n-1}}(\xi')$ are the cumulative distribution (3.10) and probability density function of that noise respectively. In this case, EVT can be applied for the n-1 remaining noise cells, which are identically distributed. They can be both expressed as

$$F_{M_{n-1}}(\xi') = \exp(-\exp(-\alpha_{n-1}(\xi' - u_{n-1}))) \tag{3.16}$$

and

$$f_{M_{n-1}}(\xi') = \alpha_n \cdot \exp(-\exp(-\xi' \cdot \alpha_n) \cdot (\exp(\alpha_n \cdot u_n) - \alpha_n \cdot \exp(\xi' \cdot \alpha_n) u_n + \alpha_n \cdot \xi' \exp(\xi' \cdot \alpha_n))) \tag{3.17}$$

where $f_{M_{n-1}}(\xi')$ was calculated by deriving $F_{M_{n-1}}(\xi')$ in Matlab.
It has to be remarked that with the expression in (3.15), it is possible to calculate the P_d by isolating different distributed terms. Once they are separated, both parts can be identified and calculated with already known statistics. When the cumulative probability of detection is defined, it is possible to get its graphical respresentation in Fig. 3.9. As it can be seen,

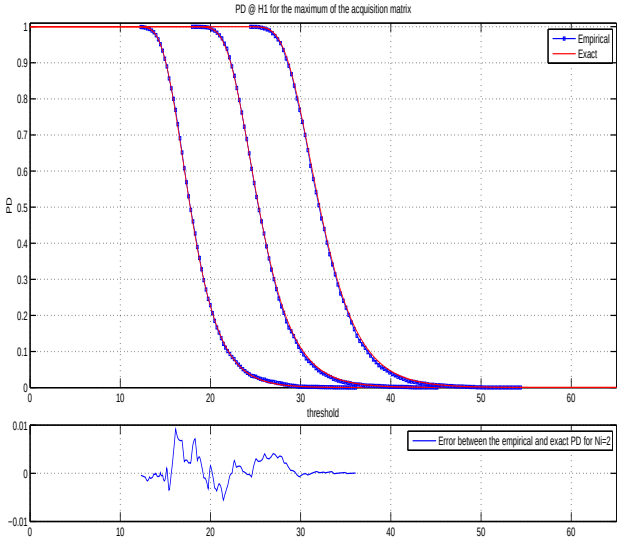

Figure 3.9: Empirical vs. exact PD's @ H1 for Multicell search with N_i={2,4,6} and C/N_0 = 30dBhz

error between exact and empirical expressions is provided for $N_i = 2$. This error magnitude is quite acceptable considering the empirical issue of having limited samples. For an improvement, more samples should be taken. However, (3.15) could be considered a good approximation for probability of detection definition.

After having defined these concepts, it is mandatory to give the ROC curve depicted in Fig. 3.11. There are some aspects to pay attention to. The first one is the error between

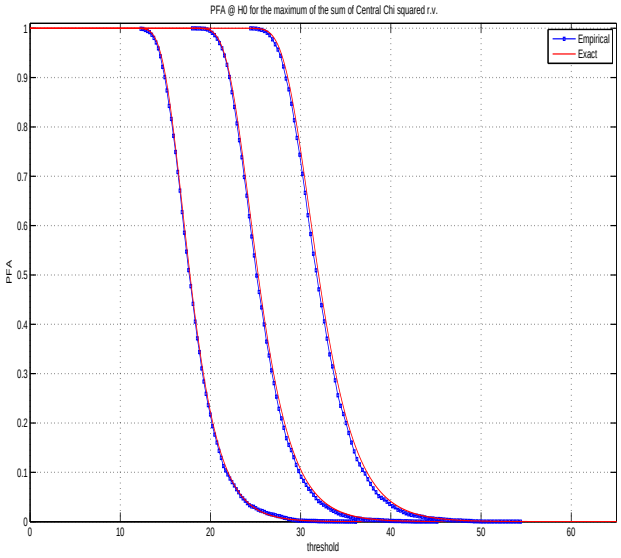

Figure 3.10: Empirical vs. exact PFA's @ H0 for Multicell search with N_i={2,4,6} and C/N_0 = 30dBhz

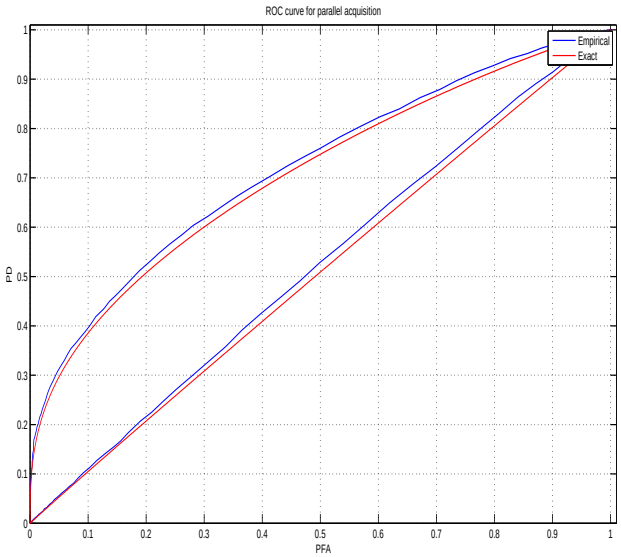

Figure 3.11: Empirical vs. exact ROC curves with N_i=4, C/N_0 = 30dBhz and Coherent integrations = {1,5}

both empirical and exact ROC which is around 0.02 when is greater. That comes from the accumulation of lower errors from distributions listed before. The second aspect to remark is

the simulation made for $N_i = 4$ and T_{cohint}=1. It has been reproduced with same parameters than Fig. 3.7 but has worse performance. That makes a lot of sense because in single cell search the probability of false alarm can only be produced by 1 noise bin which overcomes the threshold. However, in multiple search, this probability increases because there are a lot of noise bins which could possibly overcome the threshold in $\mathcal{H}_0$.

Finally, denote that increasing the coherent integration time, also benefits performance of the receiver, but has its issues.

Chapter 4

Improved signal detection based on first absolute moment

This chapter will consider the possibility to use absolute statistics instead of second-order statistics typically adopted in traditional GNSS receivers. To do so, it will discuss its performance in the simplistic and ideal case of single cell search. Once the basic statistics are defined, the practical situation of multiple cell search will be introduced.

4.1 Problem statement

A study made by a research group about delay tracking [Hur], observed an interesting result while calculating MEE (multipath error envelope). They saw that using absolute value as the nonlinear function in noncoherent acquisition tended to perform better (understood as lower errors in MEE) than the typical squaring function. Although, the researches stated that statistics describing absolute value applied in noncoherent correlators, were not available yet.

As it has been seen in Chapter 2, a HS-GNSS receiver uses noncoherent detection metrics, in order to avoid phase wrapping and changing navigation bits. That is done to have longer acquisition periods to increase the chances to detect the satellite signal. This nonlinear function is typically considered squaring the incoming value. For the case of study in this chapter, this nonlinear function is going to be the application of the absolute value to the coherent correlator output value ($y(i)$). To do so, absolute statistics have to be defined, which is one of the goals of this project.

4.2 Featuring the test variable

first-order absolute moment acquisition is going to be analysed for both paths of acquisition, single cell search and multicell search. Once their statistics are analysed, detection features as probability of detection, probability of false alarm and ROC curve will be given. The use of absolute moment while acquisition will be the main objective of this chapter.

4.3 Single cell analysis

Coming back to the GNSS block diagram in Fig. 2.7, the detection metric for the case under study becomes

$$\xi = \sum_{i=0}^{N_i-1} |y(i)| \,. \tag{4.1}$$

where $y(i)$ was the output value from the coherent correlator and N_i the number of noncoherent integrations added.

As it has been defined in Section 3.1, $y(i)$ was a random variable following $\mathcal{N}(\mu, \sigma^2)$. The output value ($\xi$) has to be analysed carefully. First, it is taken $N_i = 1$ which implies having only noncoherently integrated 1 sample. The pdf which characterizes this sample under $\mathcal{H}_0$ situation can be written as

$$f(x|\mathcal{H}_0) = \begin{cases} \frac{x}{\sigma^2}\exp(-\frac{1}{2\sigma^2}x^2) & x > 0 \\ 0 & x < 0 \end{cases} \tag{4.2}$$

More concretely, a single sample through absolute noncoherent detector under $\mathcal{H}_0$ hypothesis is a Rayleigh random variable.

On the other hand, the same single sample but under $\mathcal{H}_1$ situation, has a pdf defined as

$$f(x|\mathcal{H}_1) = \begin{cases} \frac{x}{\sigma^2}\exp[-\frac{1}{2\sigma^2}(x^2+\alpha^2)]I_0(\frac{\alpha x}{\sigma^2}) & x > 0 \\ 0 & x < 0 \end{cases} \tag{4.3}$$

Now, the output value is known as a Rician random variable. The α^2 parameter can be found as

$$\alpha^2 = \mu_1^2 + \mu_2^2 = (\frac{A}{\sqrt{2}})^2 + (j\frac{A}{\sqrt{2}})^2 = A^2 \tag{4.4}$$

where μ_1 and μ_2 are the in-phase and quadrature component means from $y(i)$ (See Section 3.1).

Once ξ distributions have been analysed for both hypothesis, we are ready to compare both empirical and exact distributions in order to be sure about the exact expressions with all parameters well-adjusted. It is very important to do so because considering a single sample is the basis to the generic case, where $N_i > 1$.

As it can be seen in Figs. 4.1 and 4.2, both empirical and exact distributions almost fit perfectly.

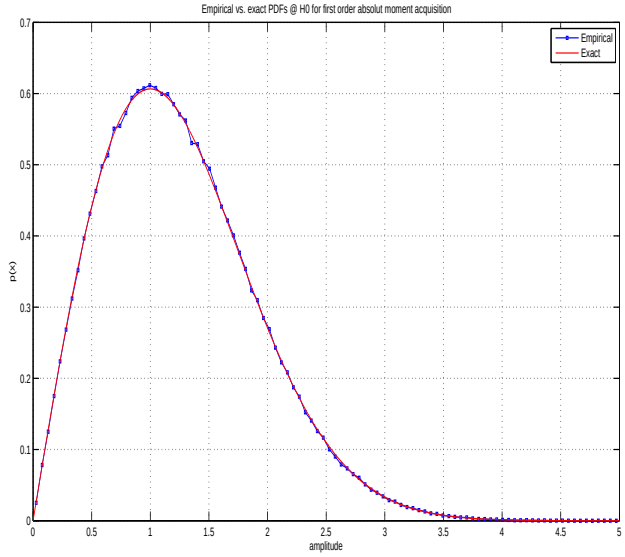

Figure 4.1: Empirical vs. exact PDF's @ H0 for first-order absolute moment acquisition with N_i=1 and C/N_0 = 35dBhz

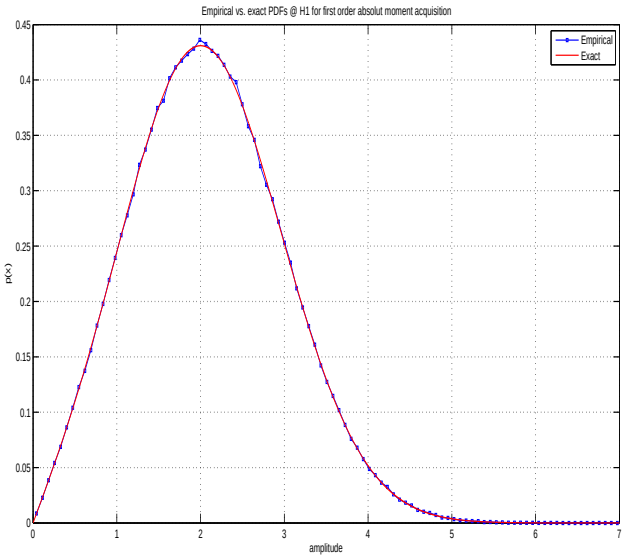

Figure 4.2: Empirical vs. exact PDF's @ H1 for first-order absolute moment acquisition with N_i=1 and C/N_0 = 35dBhz

Once single sample case has been analysed, let's face the situation where noncoherent inte-

grator adds more than one coherent correlator output samples.
As these sections are centred in single cell search, all the results will be needed to further real characterization. By their own, they are useless.

4.3.1 Analytical distribution for the sum of random variables

From [Pap91], can be found the following definition:
If two random variables are independent, then the density of their sum equals the convolution of their densities.

$$f_z(z) = \int_{x=-\infty}^{\infty} f_x(x) f_y(z-x) dx = f_x(z) * f_y(z) \tag{4.5}$$

where $f_z(x)$ is the resulting distribution of summing $f_x(x)$ and $f_y(y)$ random variables.

Values integrated in noncoherent correlator are random variables because of the noise component. This noise component is independent from other output samples from the correlator. That is why convolution can be applied. Figs. 4.3 and 4.4 gives an idea of how reliable convolution turns out to be for the sum of Rician/Rayleigh random variables.

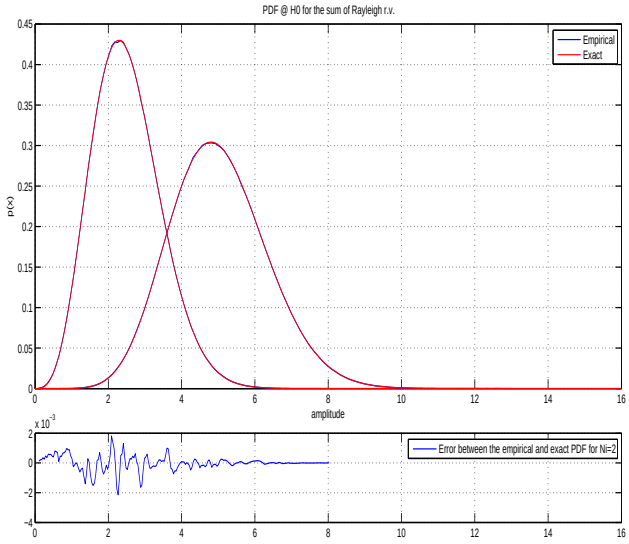

Figure 4.3: Empirical vs. exact (convolution) PDF's @ H0 with N_i={2,4} and C/N_0 = 35dBhz and error rate for $N_i = 2$

Looking at these figures, convolution method can be considered the solution about summing Rician/Rayleigh random variables, as it is the exact way to calculate the resulting sum. However, as it may be known, convolution process is quite complex so it is rather slow to obtain.

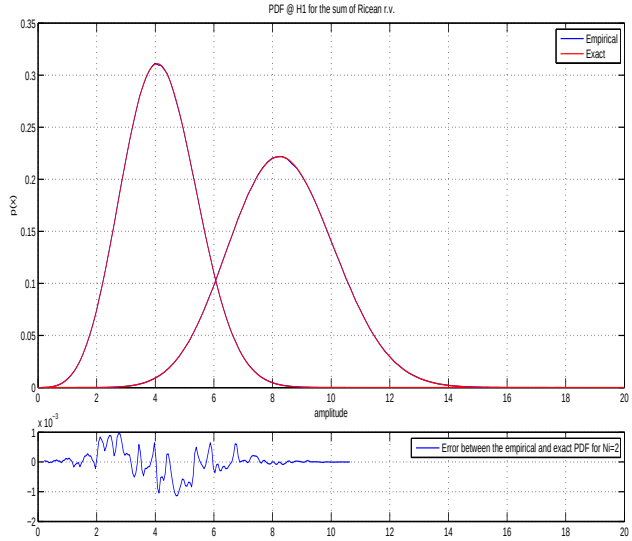

Figure 4.4: Empirical vs. exact (convolution) PDF's @ H1 with N_i={2,4} and C/N_0 = 35dBhz and error rate for $N_i = 2$

Depending on the number of noncoherent integrations, hundreds, and sometimes even thousands of convolutions may be needed. That would be the case for harsh environments, so this option is almost discarded because of its inoperability. That is why a closed-form expression would be the solution to cope with this issue.

4.3.2 Approximated distribution for the sum of random variables

A recent study [LS08a] has developed a closed-form expression for the sum of i.i.d Rice/Rayleigh random variables, based on the CLT (Central Limit Theorem) and series expansion. This expression could be very useful in order to solve the lack of results in the field of signal detection based on absolute moments.

For a large N_i, the statistical distribution for the sum of i.i.d random variables such as Rice and Rayleigh, can be represented as Gaussian in virtue of the CLT. However, sometimes this approximation is too loose when studying the tails of resultant distributions, which considerably differ from the reality. In order to fit as much as possible to the target distribution, series expansions are considered to reduce the error. This model, leads to probability density function based on Hermite polynomials as follows

$$f_\xi(\xi) = \frac{1}{\sqrt{2\pi}\sigma} e^{\frac{-(\xi-m)^2}{2\sigma^2}} [1 + \sum_{k=3}^{\infty} C_k H_k(\frac{\xi - m}{\sigma})] \tag{4.6}$$

with $\{m, \sigma\}$ the mean and variance of the detection metric ξ, $H_k(x)$ the Hermite polynomials

and C_k some coefficients related with the moments of ξ,

$$H_k(x) = (-1)^k e^{x^2/2} \frac{d^k}{dx^k} e^{-x^2/2} \tag{4.7}$$

$$C_k = \int_{-\infty}^{\infty} H_k(\xi) f_\xi(\xi) d\xi \tag{4.8}$$

The expression in (4.6) is called Gram-Charlier type-A series approximation. However, the Gram-Charlier approximation is known to be affected by poor convergence properties [Ken77]. In particular, the terms of infinite series in (4.6) do not decrease with increasing the order k, thus making the truncation of the series not so trivial. A proper arrangement of the error terms in order to get a good approximation is known as Edgeworth series of expansion, which is based on agruping the similar terms [Cra99]. For the case under study, we will consider the series expansion with terms $k = \{3, 4, 6\}$.

First of all, coefficients C_k are defined as

$$C_3 = \frac{m_{\xi,3} - 3m_{\xi,1}m_{\xi,2} + 2m_{\xi,1}^3}{6\sigma^3} \tag{4.9}$$

$$C_4 = \frac{1}{24} \frac{m_{\xi,4} - 4m_{\xi,1}m_{\xi,3} + 6m_{\xi,1}^2 m_{\xi,2} - 3m_{\xi,1}^4}{\sigma^4} - 3 \tag{4.10}$$

$$C_6 = \frac{1}{2}(C_3)^2 \tag{4.11}$$

with $m_{\xi,n} = E[\xi^n]$ the n-th moment of the detection metric ξ, defined in [LS08a](14-17) . Hermite polynomials for $k = \{3, 4, 6\}$ turns out to be

$$H_3 = x^3 - 3x \tag{4.12}$$

$$H_4 = x^4 - 6x^2 + 3 \tag{4.13}$$

$$H_6 = x^6 - 15x^4 + 45x^2 - 15 \tag{4.14}$$

Once statistics have been defined, we are ready to compare both empirical and Edgeworth series expansion distributions in order to be sure about the exact closed-form expression with all parameters well-adjusted.

As it can be seen in Figs. 4.5 and 4.6, both empirical and exact distributions almost fit perfectly. That is good news, as it seems to have been solved the problem of non having a theoretical expression for the sum of Rice/Rayleigh random variables. That will allow calculating performance metrics theoretically.

Once the verification has been done for the PDF, it is also required to double-check the tightness of the Edgeworth series expansion and empirical cumulative distribution function (CDF). As it is known, CDF can be defined as the integration of the PDF

$$F(x) = \int_{x}^{\infty} f(x) dx \tag{4.15}$$

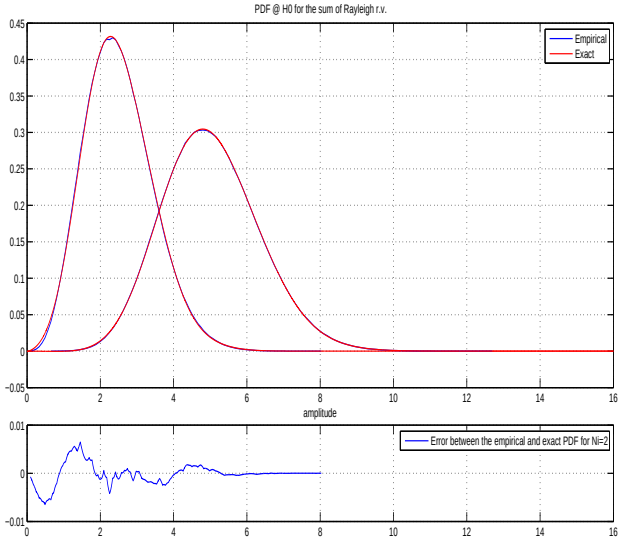

Figure 4.5: Empirical vs. exact (Edgeworth Series Expansion) PDF's @ H0 with N_i={2,4} and C/N_0 = 35dBhz and error rate for $N_i = 2$

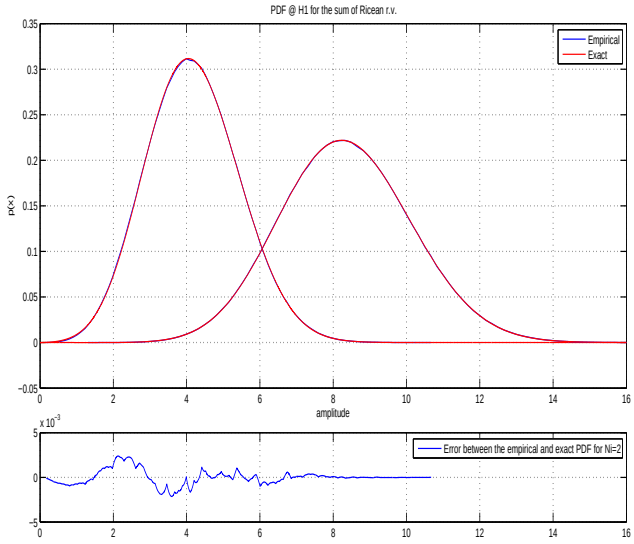

Figure 4.6: Empirical vs. exact (Edgeworth Series Expansion) PDF's @ H1 with N_i={2,4} and C/N_0 = 35dBhz and error rate for $N_i = 2$

Normally, to calculate the CDF from a multi-parameter function such as chi-square distribution is done analytically. There is no particular expression to define CDF. The closed-form expression for the sum of Rice/Rayleigh random variables in (4.6) was put through Maple to check whether it had a closed-form expression for the CDF too. Surprisingly, Maple gave an expression which

becomes

$$F_\xi(x) = -\frac{\sqrt{2}}{4\sqrt{(\pi)}}\Big(\sqrt{2\pi}(erf(\frac{x\sqrt{2}}{2})) - 2C_3e^{(-x^2/2)} + 2C_3x^2e^{(-x^2/2)} - 6C_4xe^{(-x^2/2)} + 2C_4x^3e^{(-x^2/2)} \\ +30C_6xe^{(-x^2/2)} - 20C_6x^3e^{(-x^2/2)} + 2C_6x^5e^{(-x^2/2)}\Big) + 0.5 \tag{4.16}$$

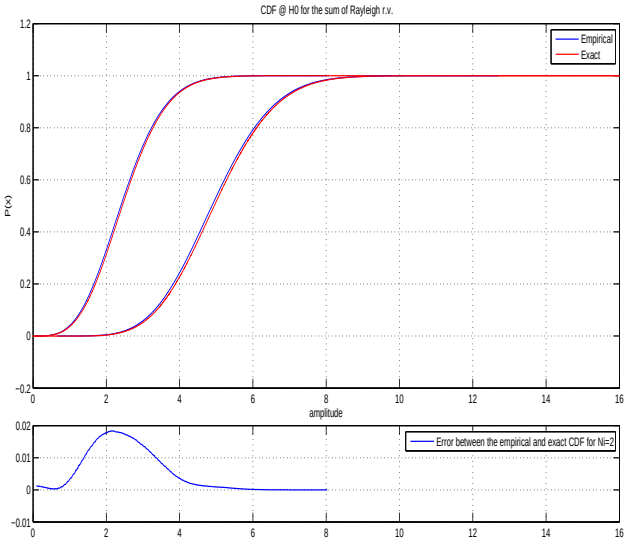

Figure 4.7: Empirical vs. exact (Edgeworth Series Expansion) CDF's @ H0 with N_i={2,4} and C/N_0 = 35dBhz and error rate for $N_i = 2$

Figs. 4.7 and 4.8 show how both empirical and exact cdfs closed-form expression fit. Looking at these figures, the Edgeworth series expansion might be considered a tight approximation although the left tail has a little deviation from the empirical target distribution. This deviation can be due to the fact that Gram-Charlier approximation is known to be affected by poor convergence properties. So the agrupation of $k = \{3, 4, 6\}$ terms may be not enough to completely make errors negligible. However, the fundamental regions which are the extremes (close to 0 and 1), the expression turns to perfectly fit again with the empirical distribution, as it can be seen thank to depicted error.

In the ROC curve, precision needs to be very tight for very small P_{fa} and high P_d because it is the zone with major interest to feature the receiver. Thus, the deviation denoted will not be of great worry.

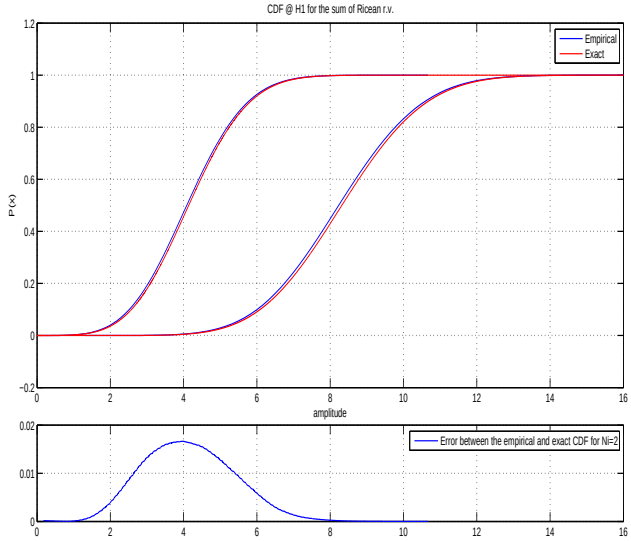

Figure 4.8: Empirical vs. exact (Edgeworth Series Expansion) CDF's @ H1 with N_i={2,4} and C/N_0 = 35dBhz and error rate for $N_i = 2$

4.3.3 Detection metrics

Detection metrics in absolute statistics turn to follow the same expressions as second-order statistics in Section 3.1.1. Only some specific terms change.

Probability of detection was already defined in Section 2.7. So the right tail integration is from the sum of Rician random variable distribution which was defined in (4.6). P_d graphical representation becomes Fig. 4.9

Probability of false alarm is also the right tail integration, now from $\mathcal{H}_0$ distribution which is the sum of Rayleigh pdfs defined by the Edgeworth series expansion in (4.6). Fig. 4.10 shows the tightness between empirical and exact P_{fa}.

Another way to calculate both P_d and P_{fa} can be

$$P_d = 1 - F_(\xi|\mathcal{H}_1) \tag{4.17}$$

$$P_{fa} = 1 - F_(\xi|\mathcal{H}_0) \tag{4.18}$$

where F_ξ is the CDF closed-form expression in (4.16) and ξ is the threshold.

Finally, the ROC curve needs to be calculated. The following figure depicted in Fig. 4.11 shows the capability of a receiver to detect satellite signal. For this case it is used a HS-GNSS applying absolute value nonlinear function while acquisition process. Again, the process made with less noncoherent integrations has not so sharper outside curvature than the process done with more samples added. Thus, they have higher P_d for same P_{fa}.

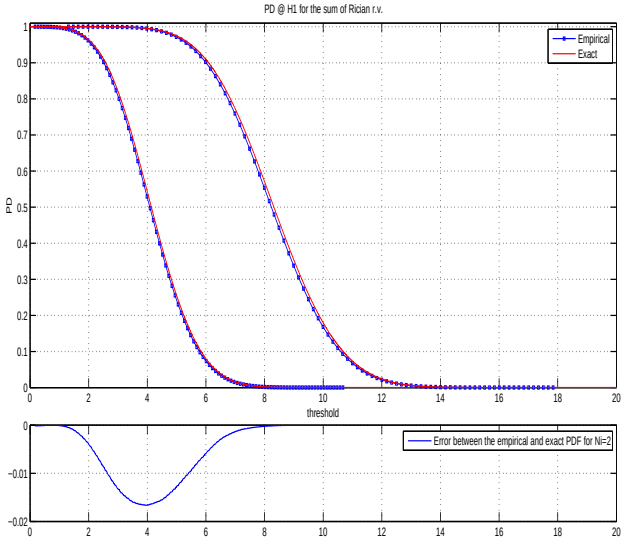

Figure 4.9: Empirical vs. exact (Edgeworth Series Expansion) PD's @ H1 with N_i={2,4} and C/N_0 = 35dBhz and error rate for $N_i = 2$

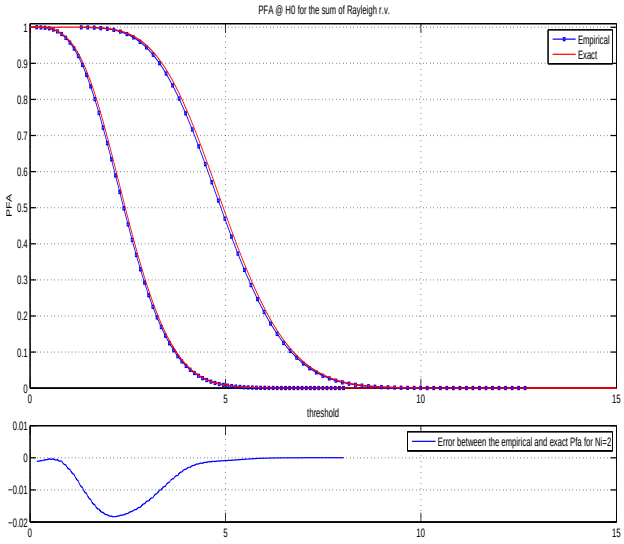

Figure 4.10: Empirical vs. exact (Edgeworth Series Expansion) PFA's @ H0 with N_i={2,4} and C/N_0 = 35dBhz and error rate for $N_i = 2$

Looking at the resulting figure, the closed-form expression for the sum of i.i.d Rice/Rayleigh random variables works almost perfectly for the case of single bin search. That is very important because all these expressions will help to characterize the real situation where the maximum output value from the acquisition matrix is picked up. The resulting error between both empirical

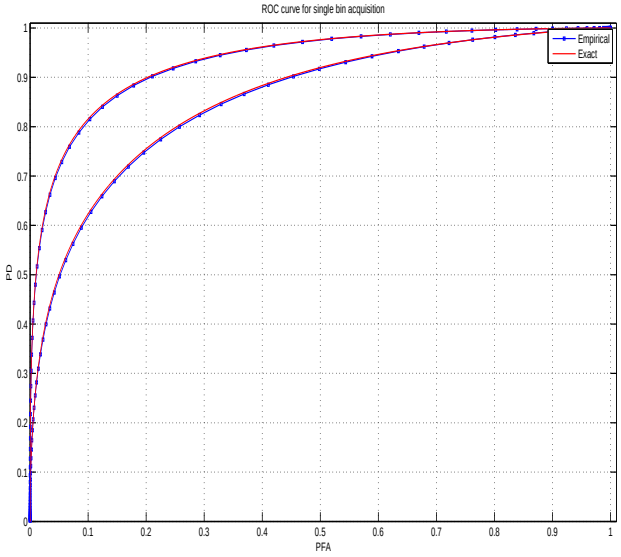

Figure 4.11: Empirical vs. exact (Edgeworth Series Expansion) ROC curves with N_i={2,4} and C/N_0 = 35dBhz

and exact curves is due to the expression proposed is not the exact one, but it fits quite tight thing that makes closed-form expressions reliable to use.

4.4 Multicell analysis

In order to be able to compare performances in Chapter 5, multicell analysis for absolute statistics must be done. That would be the actual case found in practice. The procedure is the same as the case for second-order statistics already described in Chapter 3.
Once the acquisition matrix is filled, the receiver picks the maximum value and compares it with the threshold to determine whether is under $\mathcal{H}_0$ or $\mathcal{H}_1$ hypothesis. This sample, follows an already known statistics which is under EVT.

Being under $\mathcal{H}_0$ situation and having the maximum value from the acquisition matrix (ξ'), the cumulative distribution can be found going through the EVT formulae mentioned in Section 2.6. It was defined as

$$F_n(x) = \exp(-\exp(-\alpha_n(x - u_n))) \tag{4.19}$$

where the coefficients u_n and α_n were defined by the equations

$$F(u_n) = 1 - \frac{1}{n} \tag{4.20}$$

and

$$\alpha_n = nf(u_n) \tag{4.21}$$

being $F(u_n)$ is the CDF of (ξ), evaluated in u_n defined by the Edgeworth series expansion in (4.16). n is the number of cells composing the acquisition matrix (500 in this case), and $f(u_n)$ is the $\mathcal{H}_0$ pdf evaluated in u_n and defined in (4.2).
If the resulting cumulative distribution $(F_n(\xi'))$ is depicted, turns out to be Fig. 4.12

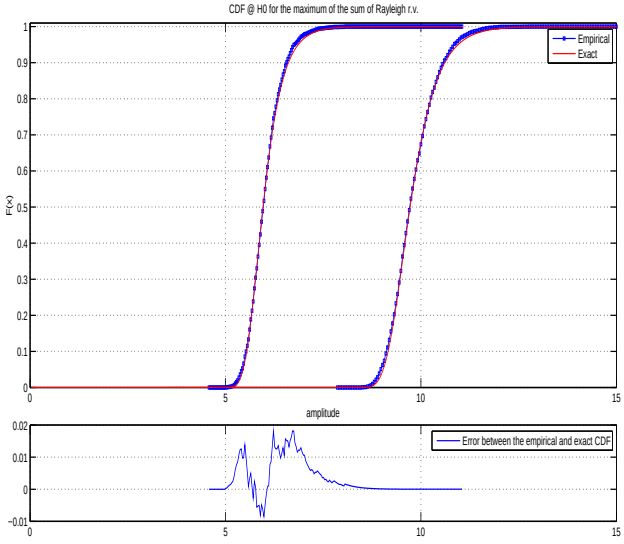

Figure 4.12: Empirical vs. exact EVT CDF's @ H0 with $N_i = \{2, 4\}$, $C/N_0 = 35$dBhz and error rate for $N_i = 2$

Using the Edgeworth series expansion also gives good results used in multicell search. In Fig. 4.12 this reliability is evident by the tightness between empirical and exact CDF. For better adjustment, more noise cells should be considered. As it was said in Section 3.2, the better adjust is found when the number of noise bins n tend to infinity, because indeed, the EVT applies asymptotically.

4.4.1 Performance metrics

Once $\mathcal{H}_0$ hypothesis is defined, probability of false alarm can be described as the right tail integration of the probability density function, or as it is the same, the CDF given by the EVT expression in (4.19).

$$P_{fa} = 1 - F_n(\xi'|\mathcal{H}_0) \tag{4.22}$$

Graphical results obtained using absolute statistics are shown in Fig. 4.13.

In order to define probability of detection, $\mathcal{H}_1$ statistics must be found. As it was seen in

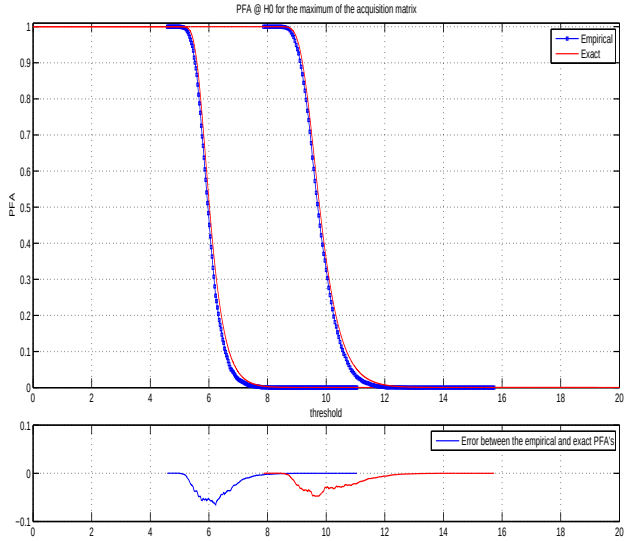

Figure 4.13: Empirical vs. exact PFA's @ H0 for Multicell search with $N_i = \{2, 4\}$, $C/N_0 =$ 35dBhz and error rate for $N_i = \{2, 4\}$

Section 3.2.1, the EVT cannot be directly applied if the receiver is under $\mathcal{H}_1$ hypothesis. The problem was that the values from the acquisition matrix were not identically distributed random variables. The cell containing signal plus noise is different distributed to the rest, making the EVT inapplicable.
Despite of that, there was a mathematical expression which helped to calculate directly the P_d that expression was

$$P_d(\gamma) = \underbrace{\int_{\gamma}^{\infty} f_{X_{sat}}(\xi')F_{M_{n-1}}(\xi')d\xi'}_{detection} + \underbrace{\int_{\gamma}^{\infty} f_{M_{n-1}}(\xi')F_{X_{sat}}(\xi')}_{misdetection} \tag{4.23}$$

where in this case, $f_{X_{sat}}(\xi')$ and $F_{X_{sat}}(\xi')$ are the pdf (4.6) and the cdf (4.16) from the signal cell. $F_{M_{n-1}}(\xi')$ and $f_{M_{n-1}}(\xi')$ are the cdf (4.19) and pdf of the $n-1$ remaining noise cells. This pdf was found in (3.17).

Isolating terms by already known expressions, P_d can be calculated. When the cumulative probability of detection is defined, it is possible to get its graphical representation in Fig. 4.14. Looking at Figs. 4.13 and 4.14, both empirical and exact curves seem to have a little deviation between them. Also it can be intuited that the more noncoherent integrations applied, the smaller the error between graphs is

Finally, the desired feature which is ROC curve can be defined. This final metric is shown in Fig. 4.15

From Fig. 4.15 it can be concluded that a receiver working under the conditions stablished

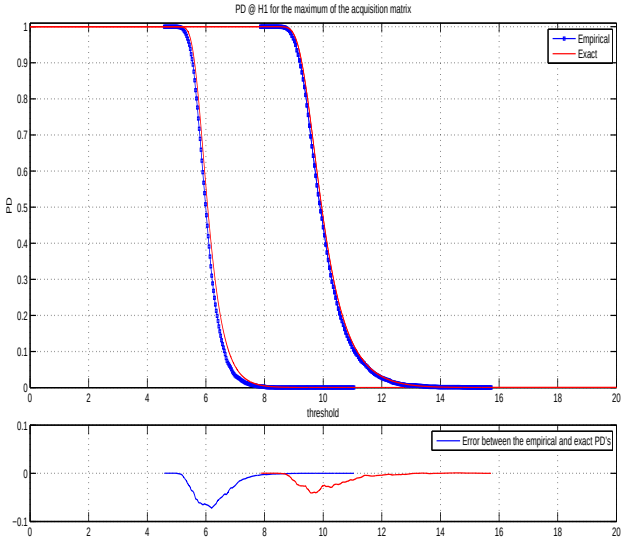

Figure 4.14: Empirical vs. exact PD's @ H1 for Multicell search with $N_i = \{2, 4\}$, $C/N_0 =$ 35dBhz and error rate for $N_i = \{2, 4\}$

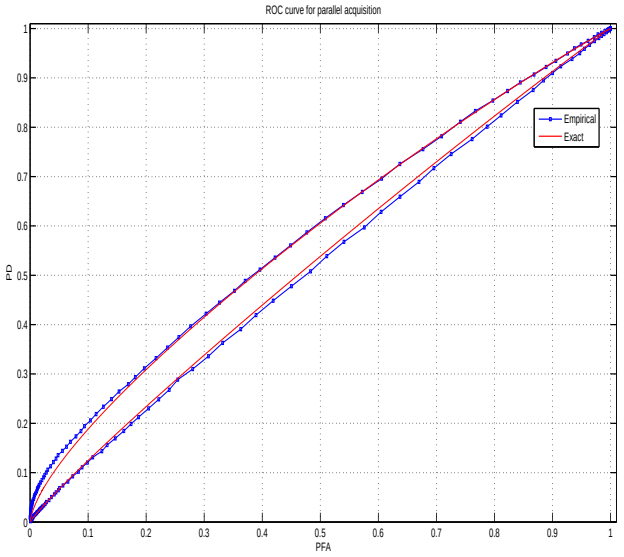

Figure 4.15: Empirical vs. exact (Edgeworth Series Expansion) ROC curves with N_i={2,4} and $C/N_0 =$ 35dBhz

($C/N_0 =$ 35dBhz) with a $T_c = 1ms$ and $N_i = \{2, 4\}$ has a poor performance. In order to have an improvement, more T_c combined with noncoherent integrations should be considered. It can be considered a good performance when PD$\approx$ 0.9 for a given PFA$\approx 10^{-6}$.

Chapter 5

Performance analysis

This final chapter will compare both first and second-order absolute statistic performances by comparing ROC curves. Changing parameters as coherent integration time, noncoherent integrations within indoor, soft indoor and outdoor scenarios will give a wide idea of the receiver's performance. As there is no possibility to have a look to all parameter combinations, a useful graph will be given in order to decide which receiver performs best in every practical situations by while providing a gain curve between both performances within the noncoherent integration range.

Before beginning with the contents, an important clarification is needed to be done. All closed-form expressions given in Chapters 2 and 3, which were a good approximation to reality, have been used to extract the results beheld in Sections 5.1 and 5.2. Apart from already well-known expressions, Edgeworth series have been used to characterize statistics for the sum of Rician/Rayleigh i.i.d variables and the probability of detection in parallel acquisition from (3.15). Indeed, they are made to be used to solve the lack of statistics in absolute value acquisition.

5.1 Single cell analysis

5.1.1 Indoor

For this first case, it has been chosen a C/N_0 within indoor scenarios range, which is 17dBhz. It will also be considered a coherent integration period of 5ms. For both detection techniques considered in this study, the one based on second-order statistics and the one based on absolute statistics, performances in terms of ROC curve is shown in Fig. 5.1

It can be observed that in order to have a good acquisition, for a 5ms coherent integration, 800 noncoherent integrations are needed. A zoom of Fig. 5.1 is shown in Fig. 5.2 in order to

highlight the different behavior of both detection techniques under analysis. As it can be seen the squared noncoherent detector outperforms the absolute one, approximately it has 2% more chances to detect satellite signal for a given PFA of 0.02.

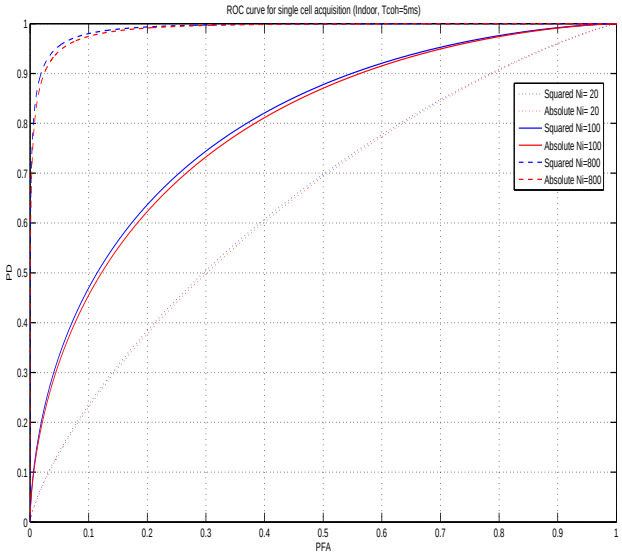

Figure 5.1: Comparision between the ROC curve for the detector based on second-order moments and the one based on absolute moments, with N_i={20,100,800} $T_{coh} = 5ms$ and $C/N_0 = 17$dBhz

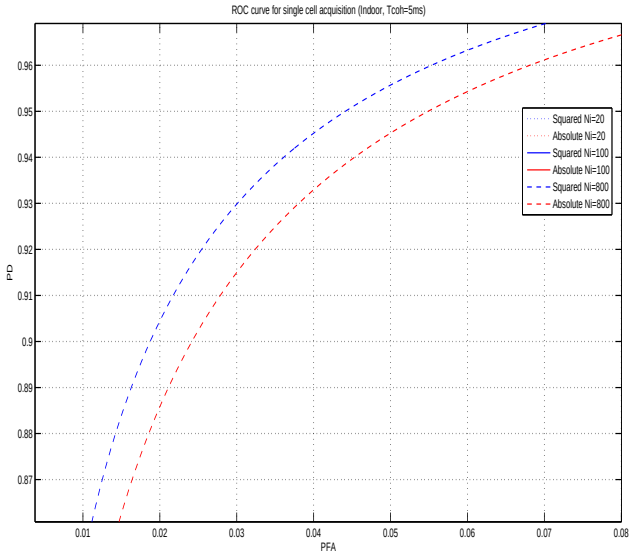

Figure 5.2: Zoom in from Fig. 5.1

We are interested to determine whether this superior performance of the second-order based detector remains for different values of noncoherent integrations. To this end, we have obtained

the gain curve comparing both acquisitions for a coherent integration time given of 5ms and varying N_i. The results are shown in Fig. 5.3.

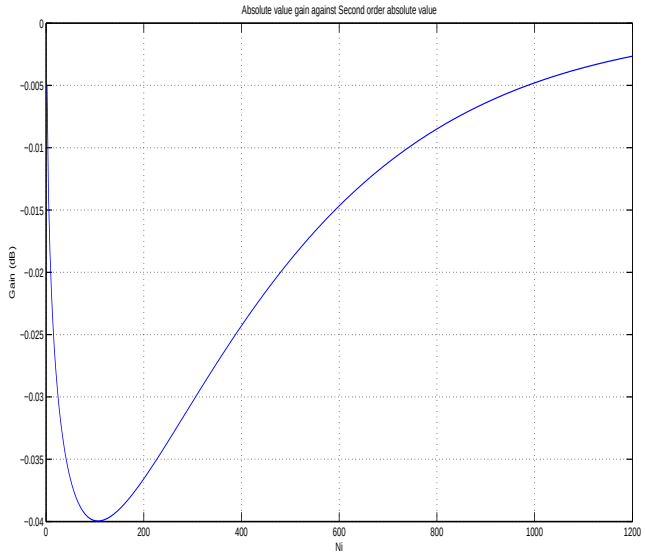

Figure 5.3: Gain curve between first and second-order absolute statistics for a $T_{coh} = 5ms$

At first sight, increasing N_i tends to stabilize both performances, but the squared acquisition seems to be better for for all values of N_i. For a good performance in this environment, it has to be considered the region with N_i greater than 800, so the gain is not very significant.

A fundamental idea might be introduced while referring to gain the curve. The maximum difference achievable between the better and the worst performances is 3dB. The best performance will be the one where both $\mathcal{H}_0$ and $\mathcal{H}_1$ distributions are enough separated to be sure whether the output value from the noncoherent correlator is under $\mathcal{H}_0$ or $\mathcal{H}_1$ hypothesis, without missing.

On the other hand, the worst performances will be the one where both $\mathcal{H}_0$ and $\mathcal{H}_1$ distributions are overlapped. That happens when the output value from the noncoherent correlator has a negligible amplitude under $\mathcal{H}_1$ which can almost be misconsidered as noise. Consequently, the right tail from $\mathcal{H}_0$ distribution will be the same as the $\mathcal{H}_1$ distribution, so P_{fa} and P_d will be the same for a given threshold value.

The difference between the best performance and the worst performance is calculated by the difference between the area under the curve. The maximum difference is found when the best performance double overcomes the worst performance. As it is known, 2 in linear becomes 3dB.

The following figure has been taken considering 10ms of coherent integration time. Performances in terms of ROC curve are shown in Fig. 5.4. From its representation could be extracted that in order to have a good performance, 300 noncoherent integrations are needed. It also can

be denoted that increasing its T_{coh}, fewer noncoherent integrations are needed for same performance as Fig. 5.1. This criterion has to be established depending on the features of the scenario because with same conditions, the study made with $T_{coh} = 1ms$ would be worse thinking about the time spent while acquisition. It would demand major number of noncoherent integrations.

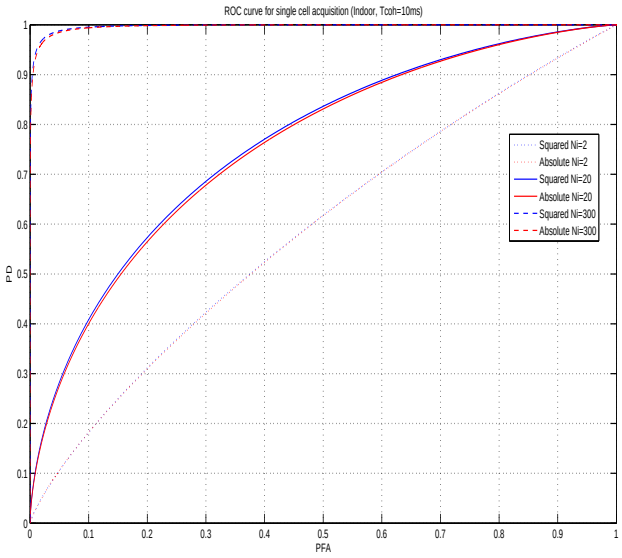

Figure 5.4: Comparision between the ROC curve for the detector based on second-order moments and the one based on absolute moments, with N_i={2,20,300} $T_{coh} = 10ms$ and $C/N_0 = 17$dBhz

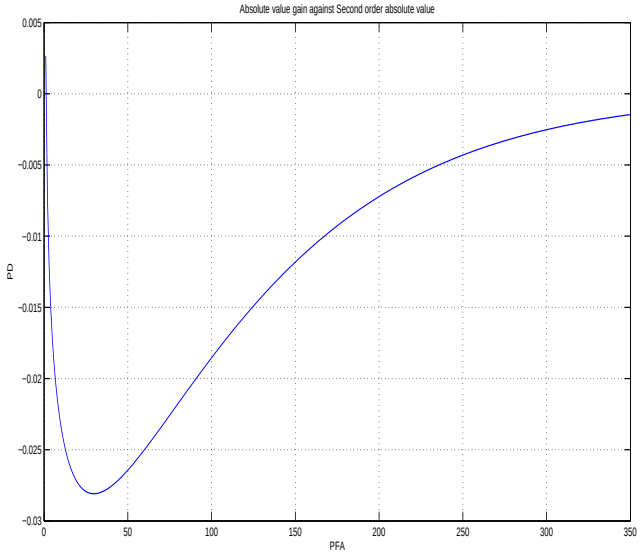

Figure 5.5: Gain curve between first and second-order absolute statistics for a $T_{coh} = 10ms$

Once the ROC curves have been analysed for the case of $T_{coh} = 5ms$, the gain curve repre-

senting the difference between performances whithin all noncoherent integration range becomes Fig. 5.5. Looking at the graph, there is a little change. The difference between performances is smaller than the case analysed in Fig. 5.3 and also tends to stabilize when looking at values of $N_i > 300$ which give a good acquisition process.

Finally, in order to have a range of different performances within indoor scenario, 20ms of T_{coh} is analysed. Performancesin terms of ROC curve are shown in Fig. 5.6.

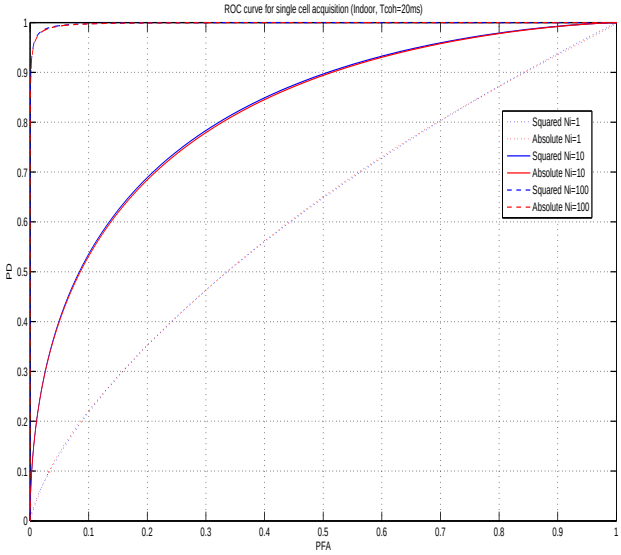

Figure 5.6: Comparision between the ROC curve for the detector based on second-order moments and the one based on absolute moments, with N_i={1,10,100} $T_{coh} = 20ms$ and $C/N_0 = 17$dBhz

As it can be seen, the consequence of increasing coherent integration and reducing the total number of noncoherent integrations to achieve a similar performance seems to have sense. Despite there is a relationship between these parameters, it is not directly proportional.
The Gain curve turns out to be Fig. 5.7. As it has been intuited, the more the coherent integration increases, the more the difference between performances decreases. This behaviour will be observed again in following scenarios, confirming the trend.

5.1.2 Soft indoor

The soft indoor scenario is now under study. Settings which characterize this environment are C/N_0, fixed at 30dBhz and $T_{coh} = 1$ms. With these first parameters set, the corresponding performances in terms of ROC curve are depicted in Fig. 5.8.

It can be seen that for $N_i = 80$, receivers have a good performance. Henceforth, every time C/N_0 increases, fewer N_i will be needed for same T_{coh}. To be able to determine whether first-

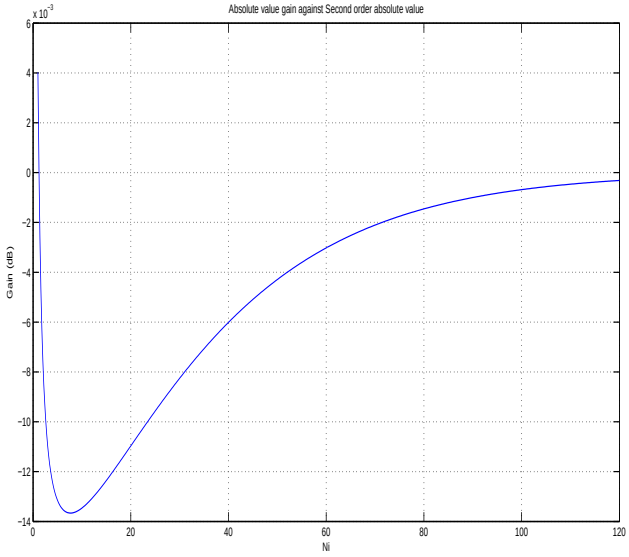

Figure 5.7: Gain curve between first and second-order absolute statistics for a $T_{coh} = 20ms$

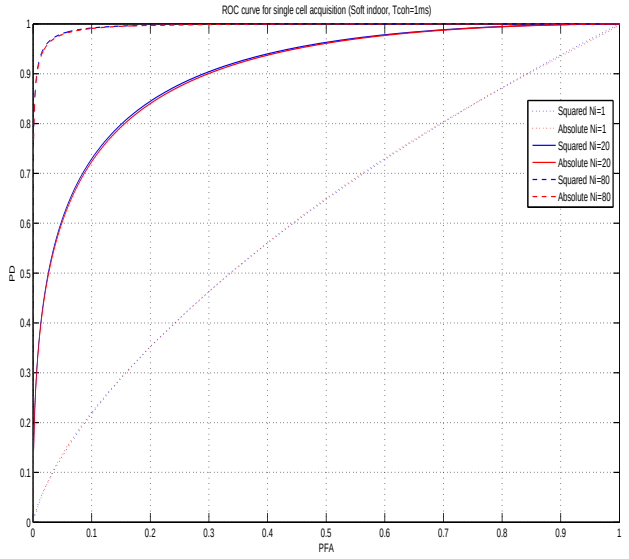

Figure 5.8: Comparision between the ROC curve for the detector based on second-order moments and the one based on absolute moments, with N_i=$\{1,20,80\}$ $T_{coh} = 1ms$ and $C/N_0 = 30$dBhz

order absolute statistics or second-order statistics perform better, gain curve is given in Fig. 5.9 for a coherent integration time given of 1ms and varying N_i.
Looking at the gain curve Fig. 5.9, the difference between performances is nearly the same of previous case in Fig. 5.7, which tend to stabilize by increasing N_i.

For both detection techniques in this study, the last soft indoor figure has been taken considering 10ms of coherent integration time. From its representation in Fig. 5.10 can be introduced a novelty from now on. Noncoherent integrations turn out to be every time less needed. That is because the amplitude from the noncoherent correlator output is greater, and only integrating it coherently is enough to have an average detection ($P_d = 0.7$ for a given $P_{fa} = 0.1$).

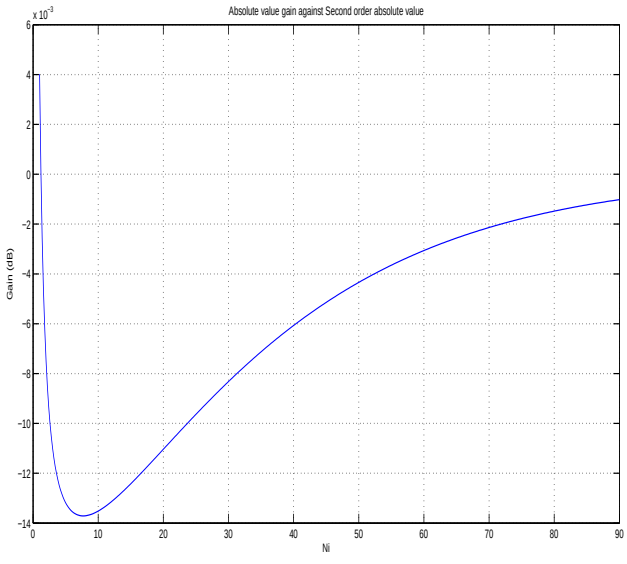

Figure 5.9: Gain curve between first and second-order absolute statistics for a $T_{coh} = 1ms$

To determine the best performance in this particular case, gain curve depicted in Fig. 5.11 is given. For the first time, the gain curve shows a different behaviour which is that absolute value barely outperforms squared one. Being aware of fitting errors between exact and empirical distributions listed before, it could be considered that they both have the same performance. Nonetheless, a change can be denoted respect previous results where squared value outperformed the absolute one.

5.1.3 Outdoor

Finally, outdoor scenario is analysed under a fixed C/N_0 of 40dBhz. For a T_{coh} of 1ms ROC curves become Fig. 5.12.

Taking a first look in it, it is easy to see that with a good signal amplitude, acquisition complexity falls. With few acquisition iterations, receivers are able to determine whether is there satellite signal or not, avoiding the majority of false alarm cases.

A zoom in is done in Fig. 5.12 to highlight the different behaviour of both detection techniques under analysis. As it can be seen in Fig. 5.13, absolute module barely outperforms the

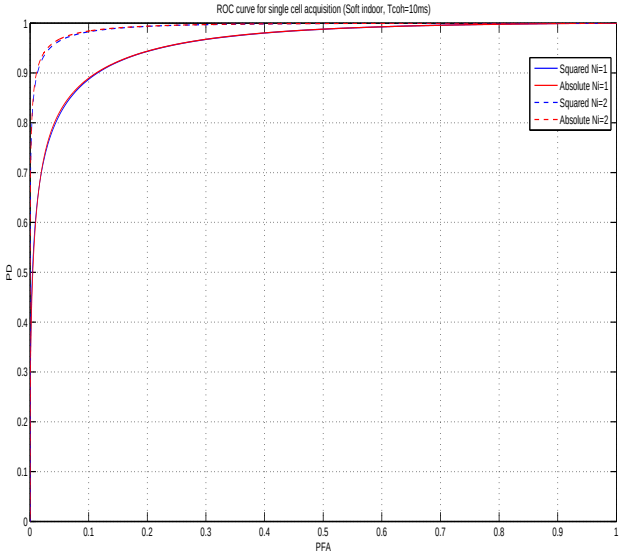

Figure 5.10: Comparision between the ROC curve for the detector based on second-order moments and the one based on absolute moments, with N_i={1,2} $T_{coh} = 10ms$ and C/N_0 = 30dBhz

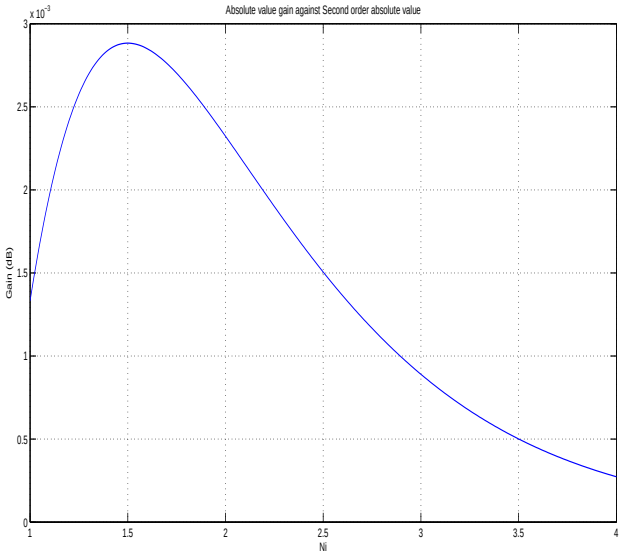

Figure 5.11: Gain curve between first and second-order absolute statistics for a $T_{coh} = 10ms$

squared one again. To this end, we have obtained the gain curve comparing both acquisitions for a coherent integration time given of 1ms and varying N_i. The results are shown in Fig. 5.14. Again, increasing N_i makes to stabilize the difference between performances.

From all results throughout this section, squared noncoherent detector turns out to perform

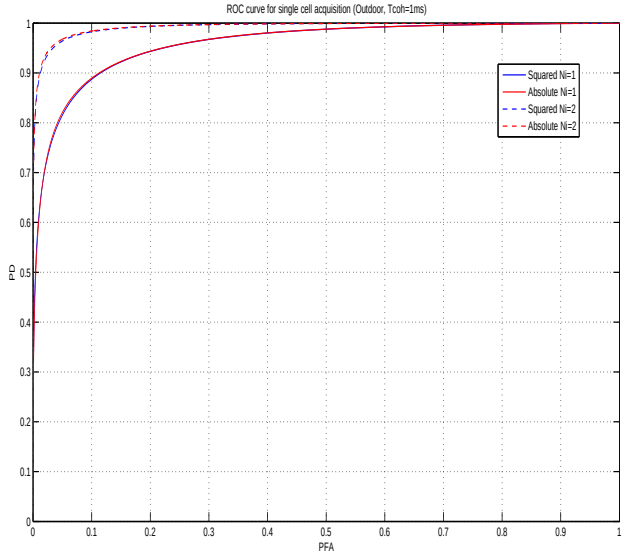

Figure 5.12: Comparision between the ROC curve for the detector based on second-order moments and the one based on absolute moments, with N_i={1,2} $T_{coh} = 1ms$ and $C/N_0 = 40$dBhz

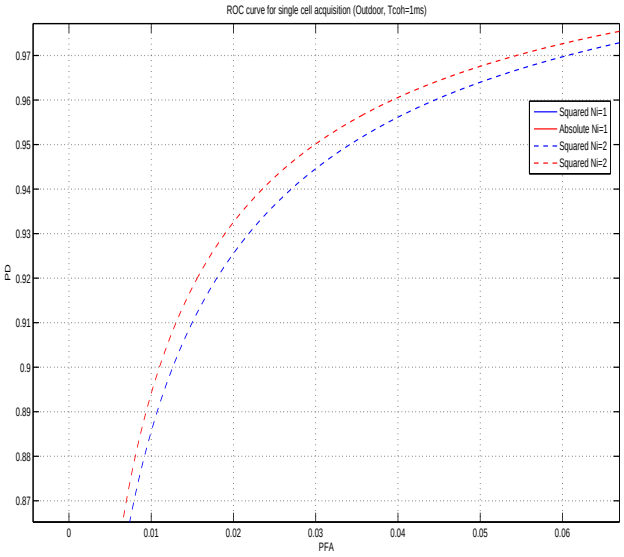

Figure 5.13: Zoom in from Fig. 5.12

better than the absoulte one for the majority of environments and parameter set. Notwithstanding, the differential gain between both performances turns to be nearly nule when noncoherently integrating many samples.

When having fewer noncoherent integrations and more coherent integration time, absolute value detector reduces its difference with squared detector and stabilizes it in more benign environ-

ments (soft indoor - outdoor).

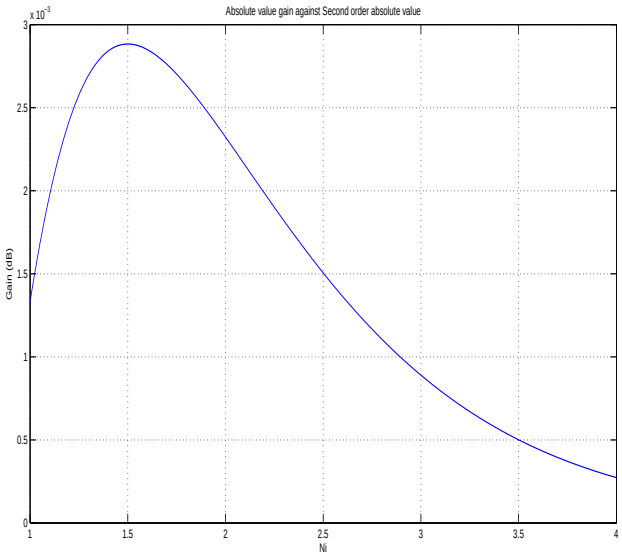

Figure 5.14: Gain curve between first and second-order absolute statistics for a $T_{coh} = 1ms$

5.2 Multicell analysis

5.2.1 Indoor

The parameter set in this first case are a C/N_0 of 17dBhz and $T_{coh} = 5$ms. For both detection techniques considered in this study, performances in terms of ROC curve are shown in Fig. 5.15. It can be seen that in order to have a good detection, N_i has to be the order of thousands. An acquisition process under this situation, cannot be operable for the given $T_{coh} = 5ms$. Theoretically it is possible, but in the reality this process cannot be held because the time spent while acquisition would be too much.

A zoom of Fig. 5.15 is shown in Fig. 5.16 in order to highlight the different behaviour of both detection techniques. It can be extracted that squared detector outperforms absolute detector quite sharply, despite it tends to stabilize for a large number of noncoherent integrations.
Gain figure in Fig. 5.17 is given to show evidences of performing differences. For a large number of noncoherent integrations, both statistics tend to stabilize but square statistics still perform better. As it can be seen, the difference between first and second-order absolute statistics still is very significant.

To have more reliable results, T_{coh} raises untill 20ms. 20ms is equivalent to the length of one transmitted bit by the satellite. If this time is exceeded, problems such as changing navigation

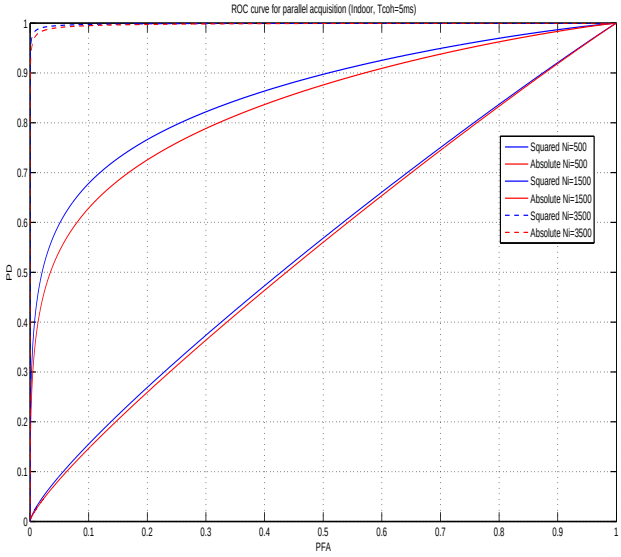

Figure 5.15: Comparision between the ROC curve for the detector based on second-order moments and the one based on absolute moments, with N_i={500,1500,3500} $T_{coh} = 5ms$ and C/N_0 = 17dBhz

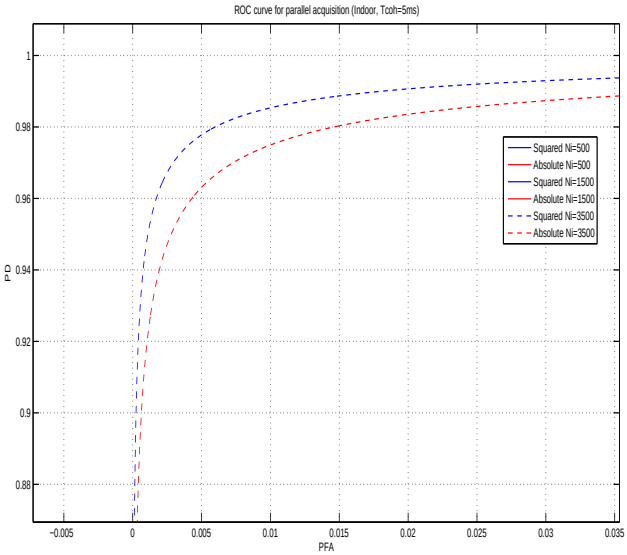

Figure 5.16: Zoom in from Fig. 5.15

bit or phase wrapping (Section 2.3.3) become present. For this second indoor analysis 20ms of coherent time is chosen. As can be observed in Fig. 5.18, performances taking $N_i > 120$ begin to be acceptable, which implies a quite high P_d for a reasonable P_{fa}. second-order statistics outperform the absolute statistics in all 3 examples shown in Fig. 5.18.

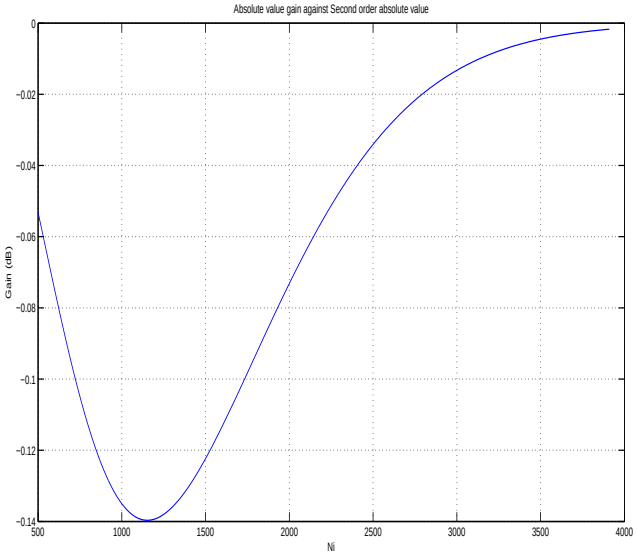

Figure 5.17: Gain curve between first and second-order absolute statistics for a $T_{coh} = 5ms$

To have an idea of the difference between statistics, Fig. 5.19 is given. Looking at Fig. 5.19, squared noncoherent detector still performs better than the first-order one for all noncoherent integrations range.

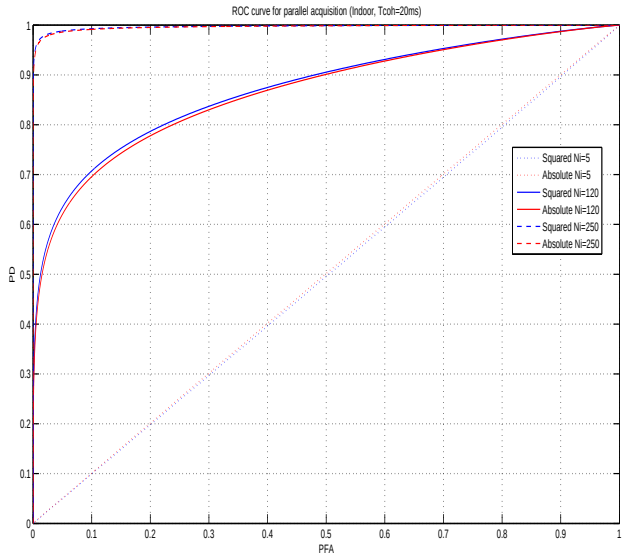

Figure 5.18: Comparision between the ROC curve for the detector based on second-order moments and the one based on absolute moments, with N_i={5,120,250} $T_{coh} = 20ms$ and $C/N_0 =$ 17dBhz

As an exception, if synchronisation is accurate and there are no phase derives, it can be

taken $T_{coh} = 40$ms. Best performance seems to change looking at ROC curve in Fig. 5.20. If a zoom in is done to the performance with $N_i = 80$, Fig. 5.21 shows that absolute noncoherent detector achieves a better result.

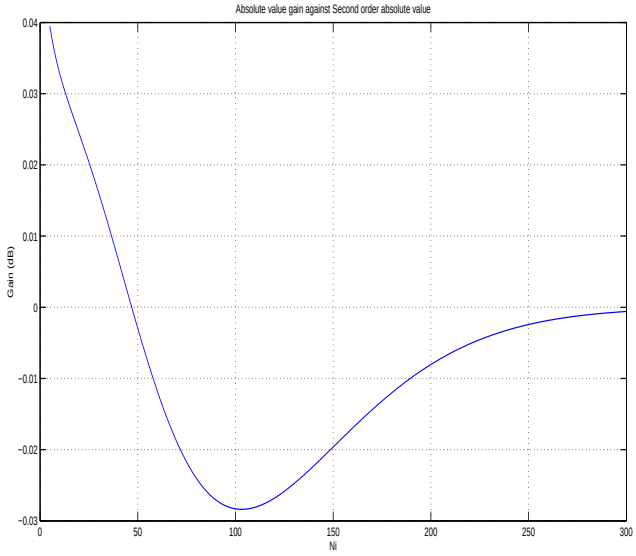

Figure 5.19: Gain curve between first and second-order absolute statistics for a $T_{coh} = 20ms$

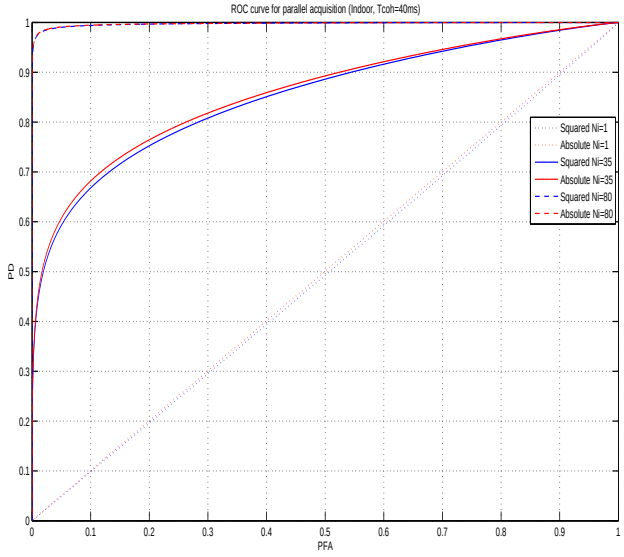

Figure 5.20: Comparision between the ROC curve for the detector based on second-order moments and the one based on absolute moments, with N_i={1,35,80} $T_{coh} = 40ms$ and $C/N_0 =$ 17dBhz

To be sure about this intuition, Fig. 5.22 is given. Looking at gain curve, can be determined

that the supposition was true for all noncoherent integration range. A coherent integration such 40ms long, apart from being better [Pan09] (if possible), seems to make first-order acquisition outperform conventional receivers.

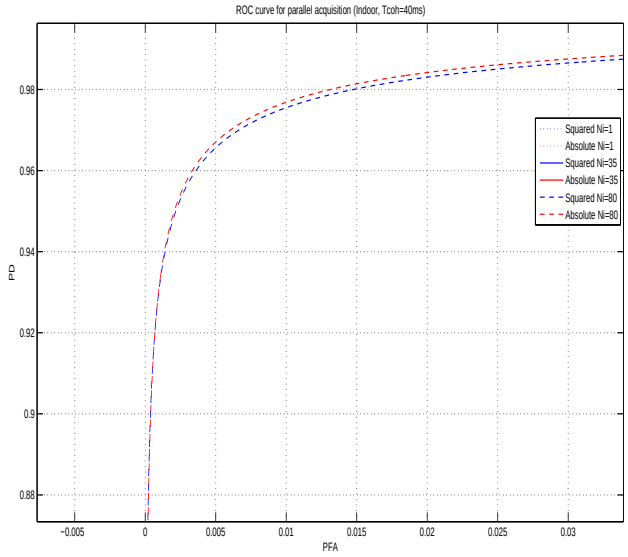

Figure 5.21: Zoom in from Fig. 5.20

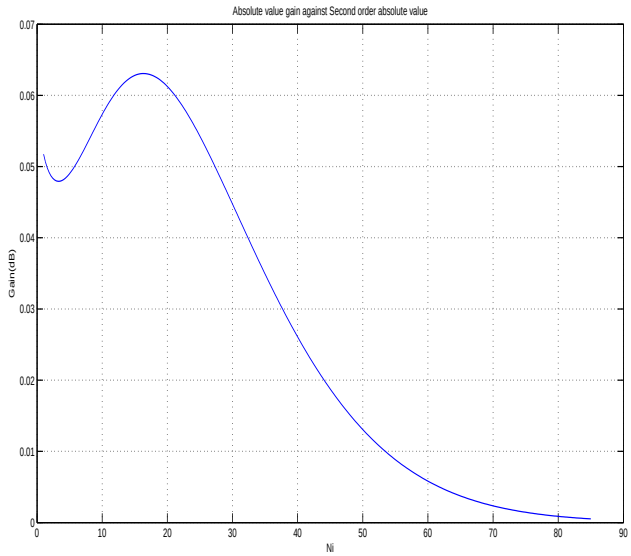

Figure 5.22: Gain curve between first and second-order absolute statistics for a $T_{coh} = 40ms$

5.2.2 Soft indoor

In this case, C/N_0 is fixed at 30dBhz. First comparision is made with $T_{coh} = 5$ms. ROC curve is depicted in Fig. 5.23) in order to see the performaces of both noncoherent detectors. With this parameter combination, the first-order detector absolutely outperforms the squared one. For high values of P_d and reasonably low for P_{fa}, this difference is noticible lower but absolute noncoherent detector still performs better.

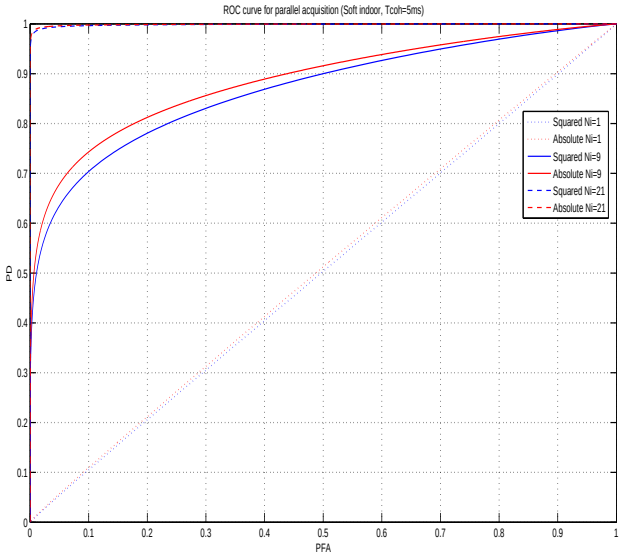

Figure 5.23: Comparision between the ROC curve for the detector based on second-order moments and the one based on absolute moments, with N_i={1,9,21} $T_{coh} = 5ms$ and $C/N_0 =$ 30dBhz

We have obtained the gain curve comparing both performances within all noncoherent integration range, depicted in Fig. 5.24. The gain curve gives evidences of this first-order absolute statistics best performance.
In order to reaffirm the outperformance of first-order detector in soft indoor environments, gain curve fixing $T_{coh} = 20$ms is analysed in Fig. 5.25.

As a result of observations made in this environment, first-order detector performs widely better than the used for conventional receivers in soft indoor scenarios. The disminution of noncoherent integrations, seems to benefy the absolute noncoherent detector.

5.2.3 Outdoor

Finally, outdoor environment is analysed in order to see whether new detector's performance still outperform the conventionals. As the amplitude is quite high ($C/N_0 = 40$dBhz), few T_{coh}

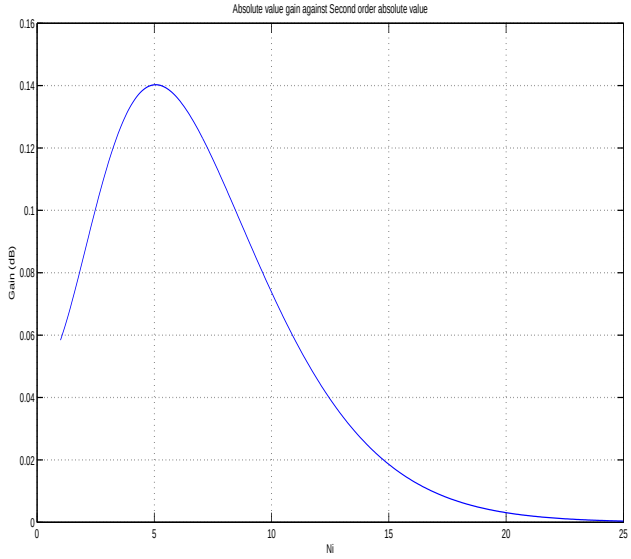

Figure 5.24: Gain curve between first and second-order absolute statistics for a $T_{coh} = 5ms$

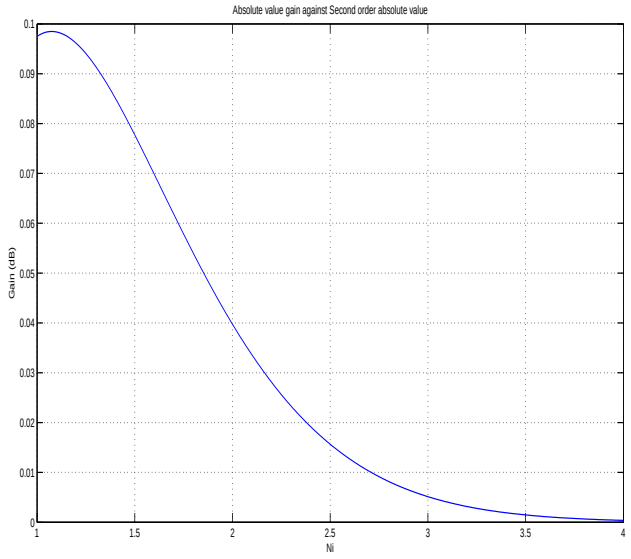

Figure 5.25: Gain curve between first and second-order absolute statistics for a $T_{coh} = 20ms$

and N_i are enough to have very satisfying results.

The case under study is taken under a $T_{coh} = 1$ms. Like the case of soft indoor scenario, the absolute value has a greater probability of detection for the same probability of false alarm in average detection, and smaller difference when having good detection as it can be seen in Fig.5.26. There are occasions where this difference increases untill five percentual points for first-order noncoherent detector.

Again, we have obtained the gain curve if Fig. 5.27 comparing both acquisitions for the T_{coh} established and all N_i range.

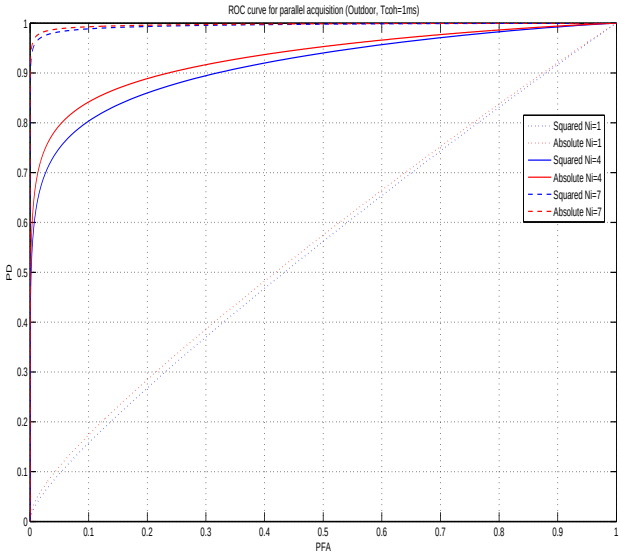

Figure 5.26: Comparision between the ROC curve for the detector based on second-order moments and the one based on absolute moments, with N_i={1,4,7} $T_{coh} = 1ms$ and C/N_0 = 40dBhz

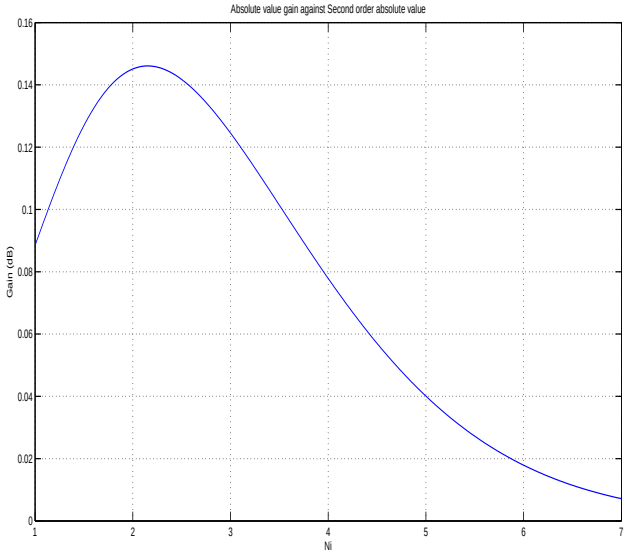

Figure 5.27: Gain curve between first and second-order absolute statistics for a $T_{coh} = 1ms$

To conclude this chapter, it has been seen that absolute value detector has a better performance rather than the squared (conventional) detector for not very harsh environments or

with the possibility to have a long coherent integration time for parallel acquisition thing which makes these results very interesting. Nonetheless, for single cell search and poor scenarios, squared noncoherent detector remains unbeaten. Table depicted in Fig. 5.28 helps to have a summary of all situations studied in this Chapter 5 and the best performing statistics in each case.

	INDOOR	SOFT INDOOR	OUTDOOR
SINGLE CELL SEARCH	Second-order statistics	Second-order statistics	Second-order statistics
MULTICELL SEARCH	Second-order statistics / First-order statistics ($T_{coh} = 40ms$)	First-order statistics	First-order statistics

Figure 5.28: Summarizing table

Chapter 6

Conclusions

To conclude this project, the results found in previous chapters are going to be presented. First of all, it has been seen that characterizing the detection process using first-order absolute statistics is possible. The first option to solve the sum of Rice/Rayleigh random variables was the convolution. This method was the exact way to calculate the resulting distribution. However, for the case of GPS detection it was inoperable because of the large acquisition time spent due to the high number of noncoherent integrations needed.
The second option was a closed-form expression based on the CLT and Edgeworth series (4.6) which turned out to be a great approximation for the sum of Rice/Rayleigh random variables. A little deviation was found in the left tail from the closed-form distribution while comparing it with the target empirical distribution. Notwithstanding, this expression could be considered a reliable way to define the sum of Rice/Rayleigh random variables. In order to reduce this little deviation, an specific study could be taken in order to make this difference negligible.

Once first and second-order noncoherent detectors were defined as well as their detection metrics, performances in terms of ROC curve were shown. From all comparisons, it was found that second-order noncoherent detectors perform best in the ideal case of single cell search and for indoor cases in parallel acquisition. However, graphical evidences have shown that the proposed first-order detector turns out to perform better in outdoor scenarios but especially in soft indoor scenarios.

From these results, it can be intuited an interesting behaviour thinking in terms of detection performance. The more coherent integrations are applied combined with few noncoherent integrations, the better the first-order noncoherent detector performs. This behaviour can be observed in indoor scenario. Although second-order statistics perform better, if it were possible to coherently integrate 40ms, first-order detector would outperform the second-order detector. That explains why first-order detector performs best in soft indoor scenarios. In these situations, coherent integrations still are very important and noncoherent integrations turn to decrease.

This combination of $10 - 20$ms of coherent integration and few noncoherent integrations is the one which most benefices the first-order noncoherent detector.

Besides, an study made by some researchers in [Pan09] have found that the more coherent integrations are taken, the more benefits the receiver has in some aspects as reducing indoor positioning problems like multipath, cross-correlation false locks, and the squaring loss. However, extending the total integration time has a price which would imply knowing the signal in order to circumvent changing navigation bits, and other issues like phase wrapping should be solved.

Having characterized first-order noncoherent detectors, a new path of investigation could be upgrading the coherent correlator to solve the limitation number of coherent integrations in order to have better results. However, first-order noncoherent detector might not be the best. Other fractional lower-order statistics could be studied and defined in order to use them in detection theory.

Bibliography

[Cra99] H. Cramer, *Mathematical Methods of Statistics*, Princeton University Press, 1999.

[Dig09] F. Van Diggelen, *A-GPS: Assisted GPS, GNSS, and SBAS*, Artech-House, 2009.

[D.K06] Elliott D.Kaplan, Christopher J.Hegarty, *Understanding GPS: principles and applications*, Artech House, Boston, 2nd ed., 2006.

[Ega75] J. E. Egan, *Signal Detection Theory and ROC analysis*, Series in Cognitition and Perception, Academic Press, New York, 1975.

[Emb97] P. Embrechts, C. Klüppelberg, T. Mikosch, *Modelling Extremal Events for Insurance and Finance*, Springer-Verlag, 1997.

[Hur] H. Hurskainen, E. Simona Lohan, X. Hu, J. Raasakka, J. Nurmi, "Multiple gate delay tracking structures for gnss signals and their evaluation with simulink, systemc, and vhdl", *International Journal of Navigation and Observation*, Vol. 2008, pags. 17.

[Kay98] S. M. Kay, *Fundamentals of Statistical Signal Processing. Detection Theory.*, Vol. II, Prentice Hall, Upper Saddle River, NJ, 1998.

[Ken77] M. G. Kendall, A. Stuart, *The Advanced Theory of Statistics*, Macmillan, New York, 1977.

[LS08a] J. A. López-Salcedo, "On the application of edgeworth series expansions to signal detection in gnss receivers, manuscript in preparation", 2008, manuscript in preparation.

[LS08b] J. A. López-Salcedo, J. López Vicario, G. Seco-Granados, "Optimal noncoherent detector for hs-gnss receivers", *International Workshop on Signal Processing for Space Communications (SPSC)*, Oct 06 2008.

[Pan09] T. Pany, B.Riedl, J. Winkel, T. Wörz, R. Schweikert, H. Niedermeier, S. Lagrasta, G. López-Risueño, D. Jiménez-Baños, "Coherent integration time: The longer, the better", *InsideGNSS*, pags. 52–61, November/December 2009.

[Pap91] A. Papoulis, *Probability, Random Variables and Stochastic Processes*, McGraw-Hill, 1991.

[Pet97] B. B. Peterson, D. Bruckner, , S. Heye, *Measuring GPS Signals Indoors*, Proc. Institute of Navigation (ION), November 1997.

[Roi03] O. Sallent Roig, J. Luis Valenzuela González, R. Agustí Comes, *Principios de comunicaciones móviles*, Edicions UPC, 2003.

[Tsu05] James Bao-Yen Tsui, *Fundamentals of global positioning system receivers, a software approach*, John Wiley & Sons, inc., publication, 2nd ed., 2005.

[Tur07] S. Turunen, "Network assistance. what will new gnss signals bring to it?", *InsideGNSS*, pags. 35–41, Spring 2007.

Resum:

Aquest projecte es centra principalment en el detector no coherent d'un GPS. Per tal de caracteritzar el procés de detecció d'un receptor, es necessita conèixer l'estadística implicada. Pel cas dels detectors no coherents convencionals, l'estadística de segon ordre intervé plenament. Les prestacions que ens dóna l'estadística de segon ordre, plasmada en la ROC, són prou bons tot i que en diferents situacions poden no ser els millors. Aquest projecte intenta reproduir el procés de detecció mitjançant l'estadística de primer ordre com a alternativa a la ja coneguda i implementada estadística de segon ordre. Per tal d'aconseguir-ho, s'usen expressions basades en el Teorema Central del Límit i de les sèries Edgeworth com a bones aproximacions. Finalment, tant l'estadística convencional com l'estadística proposada són comparades, en termes de la ROC, per tal de determinar quin detector no coherent ofereix millor prestacions en cada situació.

Resumen:

Este proyecto se centra básicamente en el receptor no coherente de un GPS. Con tal de caracterizar el proceso de detección de un receptor, es necesario conocer la estadística implicada. En el caso de los detectores no coherentes convencionales, la estadística de segundo orden interviene plenamente. Los resultados que nos da esta estadística, plasmada en la curva ROC, son bastante satisfactorios aunque en distintos escenarios pueden no ser los mejores. Este proyecto intenta reproducir el proceso de detección mediante la estadística de primer orden como alternativa a la ya conocida e implementada estadística de segundo orden. Con tal de conseguirlo, se van a usar expresiones basadas en el Teorema Central del Límite y de las series Edgeworth como aproximaciones fiables. Finalmente, tanto la estadística propuesta como la estadística convencional son comparadas, en términos de la curva ROC, con tal de determinar cual detector no coherente ofrece mejores prestaciones en cada situación.

Summary:

This project focuses in GPS noncoherent detectors. In order characterize detection metrics from a receiver, statistics are demanded to be known. For the case of conventional noncoherent detectors, second-order statistics play an important role. The detection performance in terms of ROC curve gives satisfying results. However, using second-order statistics does not give the best performance in different environmental situations. This project tries to characterize detection metrics using first-order statistics as an alternative to conventional second-order statistics. To do so, some closed-form expressions based in the Central Limit Theorem and the Edgeworth series will be used as a good approximation. Finally, they are both compared to determine the best noncoherent detector for each situation.